Relationship between inflammatory periarteritis and IgG4-SD

Inoue et al. demonstrated 17 cases of inflammatory periaortitis or periarteritis that had occurred in the superior mesenteric, inferior mesenteric, and splenic arteries [60], and histologic examination of which, when available, revealed irregular fibrosis in the arterial walls and diffuse infiltration of IgG4-positive cells within the inflamed areas. In addition, Matsumoto et al. presented a case of IgG4-related abdominal periaortitis and inflammatory coronary periarteritis, manifested as a tumorous mass around the coronary artery [17]. Furthermore, we have recently experienced a patient with IgG4-related periarteritis of the coronary artery who was admitted to our hospital owing to the chest symptoms [23]. In this patient, serum IgG4 levels were elevated at 564 mg/dL, and a glittery white-yellowish elastic-hard periarterial mass surrounding the left circumflex artery could be seen after the incision of the pericardium. Whether IgG4-related coronary periarteritis plays a role in the development of coronary artery stenosis remains to be investigated, however, we may have to be, at least, aware that coronary periarteritis may increasingly be diagnosed in the era of multi-detector coronary-CT angiography.

Inflammatory pericarditis and IgG4-SD

Several reports have demonstrated inflammatory pericardial fibrosis that occurred as a manifestation of systemic multifocal fibrosclerosis [2,24]. Sugimoto et al. reported a 68-year-old man who showed constrictive pericarditis as the initial manifestation, and staining of the excised pericardium with anti-IgG4 antibody revealed the infiltration of IgG4-positive plasma cell [61]. This patient developed pleural effusion and progressive pleural fibrosis six months after post-pericardiostomy. We have recently reported an 83-year-old man with pericardial fibrosis who died from cardio-respiratory failure due to massive pericardial effusion, and autopsy showed the infiltration of IgG4-positive plasma cells in the pericardium, as well as in the visceral and parietal pleura, pancreas, and retroperitoneal fibrous tissues [45]. This patient had a past history of autoimmune pancreatitis. These observations were consistent with the notion that inflammatory pericarditis may also develop as a feature of IgG4-related multifocal fibrosclerosis.

Fibroinflammatory disorders of myocardium

Whether IgG4-related immuno-inflammation may underlie myocardial fibrosclerosis that would lead to cardiac failure seems to have been least extensively studied [62,63]. Cardiac sarcoidosis may be one of the disorders associated with the infiltration of lymphocytic cells and development of fibrosis in the heart [64]. We investigated the relationship between IgG4-SD and cardiac sarcoidosis; however, we could not find a meaningful relationship between these conditions [65]. Whether IgG4-related immuno-inflammation would underlie the pathogenesis of other myocardial disorders causing fibrosis and cardiac failure should be assessed in further studies.

Hurdles to overcome for further investigations

As discussed above, IgG4-related autoimmunity may, although not always, underlie multifocal fibrosclerosis in the cardiovascular system. Toward achieving optimal therapeutic strategies and better understanding of the pathophysiology of IgG4-related fibrosclerosis in the cardiovascular system, there is an increasing need for research in this field; however, there are several hurdles to overcome before advances can be made.

First, the definition, as well as the nomenclature, of the disorder. Inflammatory aortic aneurysm is said to be present when periaortic fibrosis coexists with dilatation of the aorta; however, the cut-off value of aortic diameter that discriminates between idiopathic retroperitoneal fibrosis and inflammatory abdominal aortic aneurysm does not seem to be clear [34], or may sometimes be impractical. Likewise, retroperitoneal fibrosis may be subclassified as *IgG4-related* and *non-IgG4-related* forms; alternatively, however, it may also be subclassified as *idiopathic* and *secondary* forms. Furthermore, because IgG4-related fibrosclerosis can also occur in small-size vessels, pericardium, and possibly pleura, it might more suitably be termed 'IgG4-related (peri)vasculitis/serositis' (Fig. 3).

Second, differential diagnosis. In infected, or mycotic, aortic aneurysm, the bacterial culture may be negative in half of all cases [66] and serum IgG4 levels might be elevated [67]. Considering that about half of all cases of inflammatory aortic aneurysm may be IgG4-related [29], these situations may make differential diagnosis between inflammatory and infected aneurysm difficult. In addition, it should also be noted that diagnosis of IgG4-related or non-IgG4-related multifocal fibrosclerosis should not be made solely depending on the responsiveness to medical therapy, because some types of malignancy that might underlie or be misdiagnosed as fibrosclerotic disorders may also respond to corticosteroid therapy [68]. In patients with multiorgan fibrosis, we should not overlook the possibility of malignant disease.

Third, IgG4 positivity. Clinical pictures and therapeutic responsiveness of non-IgG4-related fibrosclerosis may be similar, sometimes almost identical, to IgG4-SD. It is possible that IgG4-positive cell infiltration may be a transient phenomenon during the development of fibrosclerotic tissue degeneration and that IgG4 may not play a central, but rather a bystander, role in the lesion formation.

Conclusion

The cardiovascular system may be one of the target organs of IgG4-related, and non-IgG4-related, systemic multifocal fibrosclerosis. Cardiologists should be aware of this clinicopathological condition, not only because it can be potently managed by corticosteroid and/or immunosuppressive therapies, but also because it can take a rapid and fatal clinical course [45]. In addition, caution should be applied because cardiovascular fibrosclerosis may be accompanied by or misdiagnosed from other co-morbidities such as infection and malignancy. Further research is warranted in the field of IgG4-related cardiovascular fibrosclerosis.

Please cite this article in press as: Ishizaka N, et al. Multifocal fibrosclerosis and IgG4-related disease involving the cardiovascular system. J Cardiol (2012), doi:10.1016/j.jjcc.2011.10.005

Acknowledgments

The work was supported in part by Health Sciences Research Grants of The Ministry of Health, Labour and Welfare of Japan (Research on Hepatitis, Acute Aortic Syndrome), Grants from Meiji Yasuda Life Foundation of Health and Welfare, Mitsui Life Social Welfare Foundation, and the Japan Society for the Promotion of Science (JSPS) through its "Funding Program for World-Leading Innovative R&D on Science and Technology (FIRST Program)."

References

[1] Sassa H, Kondo J, Tsuboi H, Sone T, Tsubone M. A case of idiopathic retroperitoneal fibrosis with chronic pericarditis. Intern Med 1992;31:414–7.
[2] Baur M, Hulla W, Kienzer H, Klimpfinger M, Dittrich C. Pericarditis as the initial manifestation of retroperitoneal fibrosis – a case report. Wien Med Wochenschr 2002;152:230–2.
[3] van der Zee JS, van Swieten P, Aalberse RC. Inhibition of complement activation by IgG4 antibodies. Clin Exp Immunol 1986;64:415–22.
[4] Hamano H, Kawa S, Horiuchi A, Unno H, Furuya N, Akamatsu T, Fukushima M, Nikaido T, Nakayama K, Usuda N, Kiyosawa K. High serum IgG4 concentrations in patients with sclerosing pancreatitis. N Engl J Med 2001;344:732–8.
[5] Hamano H, Kawa S, Ochi Y, Unno H, Shiba N, Wajiki M, Nakazawa K, Shimojo H, Kiyosawa K. Hydronephrosis associated with retroperitoneal fibrosis and sclerosing pancreatitis. Lancet 2002;359:1403–4.
[6] Smyrk TC. Pathological features of IgG4-related sclerosing disease. Curr Opin Rheumatol 2011;23:74–9.
[7] Zen Y, Nakanuma Y. IgG4-related disease: a cross-sectional study of 114 cases. Am J Surg Pathol 2010;34:1812–9.
[8] Van Moerkercke W, Verhamme M, Doubel P, Meeus G, Oyen R, Van Steenbergen W. Autoimmune pancreatitis and extrapancreatic manifestations of IgG4-related sclerosing disease. Acta Gastroenterol Belg 2010;73:239–46.
[9] Okazaki K, Uchida K, Koyabu M, Miyoshi H, Takaoka M. Recent advances in the concept and diagnosis of autoimmune pancreatitis and IgG4-related disease. J Gastroenterol 2011;46:277–88.
[10] Takato H, Yasui M, Ichikawa Y, Fujimura M, Nakao S, Zen Y, Minato H. Nonspecific interstitial pneumonia with abundant IgG4-positive cells infiltration, which was thought as pulmonary involvement of IgG4-related autoimmune disease. Intern Med 2008;47:291–4.
[11] Saeki T, Saito A, Hiura T, Yamazaki H, Emura I, Ueno M, Miyamura S, Gejyo F. Lymphoplasmacytic infiltration of multiple organs with immunoreactivity for IgG4: IgG4-related systemic disease. Intern Med 2006;45:163–7.
[12] Umemura T, Zen Y, Hamano H, Ichijo T, Kawa S, Nakanuma Y, Kiyosawa K. IgG4 associated autoimmune hepatitis: a differential diagnosis for classical autoimmune hepatitis. Gut 2007;56:1471–2.
[13] Yamamoto M, Takahashi H, Sugai S, Imai K. Clinical and pathological characteristics of Mikulicz's disease (IgG4-related plasmacytic exocrinopathy). Autoimmun Rev 2005;4:195–200.
[14] Leporati P, Landek-Salgado MA, Lupi I, Chiovato L, Caturegli P. IgG4-related hypophysitis: a new addition to the hypophysitis spectrum. J Clin Endocrinol Metab 2011;96:1971–80.
[15] Dahlgren M, Khosroshahi A, Nielsen GP, Deshpande V, Stone JH. Riedel's thyroiditis and multifocal fibrosclerosis are part of the IgG4-related systemic disease spectrum. Arthritis Care Res (Hoboken) 2010;62:1312–8.
[16] Stone JH, Khosroshahi A, Deshpande V, Stone JR. IgG4-related systemic disease accounts for a significant proportion of thoracic lymphoplasmacytic aortitis cases. Arthritis Care Res (Hoboken) 2010;62:316–22.
[17] Matsumoto Y, Kasashima S, Kawashima A, Sasaki H, Endo M, Kawakami K, Zen Y, Nakanuma Y. A case of multiple immunoglobulin G4-related periarteritis: a tumorous lesion of the coronary artery and abdominal aortic aneurysm. Hum Pathol 2008;39:975–80.
[18] Neild GH, Rodriguez-Justo M, Wall C, Connolly JO. Hyper-IgG4 disease: report and characterisation of a new disease. BMC Med 2006;4:23.
[19] Zen Y, Kitagawa S, Minato H, Kurumaya H, Katayanagi K, Masuda S, Niwa H, Fujimura M, Nakanuma Y. IgG4-positive plasma cells in inflammatory pseudotumor (plasma cell granuloma) of the lung. Hum Pathol 2005;36:710–7.
[20] Zen Y, Fujii T, Sato Y, Masuda S, Nakanuma Y. Pathological classification of hepatic inflammatory pseudotumor with respect to IgG4-related disease. Mod Pathol 2007;20:884–94.
[21] Mitchinson MJ, Wight DG, Arno J, Milstein BB. Chronic coronary periarteritis in two patients with chronic periaortitis. J Clin Pathol 1984;37:32–6.
[22] Mitchinson MJ. Chronic periaortitis and periarteritis. Histopathology 1984;8:589–600.
[23] Tanigawa J, Daimo M, Murai M, Katsumata T, Tsuji M, Ishizaka N. IgG4-related coronary periarteritis in patients presenting with myocardial ischemia. Hum Pathol, in press.
[24] Omura Y, Yoshioka K, Tsukamoto Y, Maeda I, Morikawa T, Konishi Y, Inoue T, Sato T. Multifocal fibrosclerosis combined with idiopathic retro-peritoneal and pericardial fibrosis. Intern Med 2006;45:461–4.
[25] Vaglio A, Buzio C. Chronic periaortitis: a spectrum of diseases. Curr Opin Rheumatol 2005;17:34–40.
[26] Kermani TA, Crowson CS, Achenbach SJ, Luthra HS. Idiopathic retroperitoneal fibrosis: a retrospective review of clinical presentation, treatment, and outcomes. Mayo Clin Proc 2011;86:297–303.
[27] Yin MD, Zhang J, Wang SY, Duan ZQ, Xin SJ. Inflammatory abdominal aortic aneurysm: clinical features and long term outcome in comparison with atherosclerotic abdominal aortic aneurysm. Chin Med J 2010;123:1255–8.
[28] Vaglio A, Corradi D, Manenti L, Ferretti S, Garini G, Buzio C. Evidence of autoimmunity in chronic periaortitis: a prospective study. Am J Med 2003;114:454–62.
[29] Kasashima S, Zen Y, Kawashima A, Konishi K, Sasaki H, Endo M, Matsumoto Y, Kawakami K, Kasashima F, Moriya M, Kimura K, Ohtake H, Nakanuma Y. Inflammatory abdominal aortic aneurysm: close relationship to IgG4-related periaortitis. Am J Surg Pathol 2008;32:197–204.
[30] Yoshizaki T, Tabuchi N, Makita S. Inferior vena cava occlusion secondary to an inflammatory abdominal aortic aneurysm. Interact Cardiovasc Thorac Surg 2007;6:128–9.
[31] Adler S, Lodermeyer S, Gaa J, Heemann U. Successful mycophenolate mofetil therapy in nine patients with idiopathic retroperitoneal fibrosis. Rheumatology (Oxford) 2008;47:1535–8.
[32] Ormond JK. Bilateral ureteral obstruction due to envelopment and compression by an inflammatory retroperitoneal process. J Urol 1948;59:1072–9.
[33] Albarran J. Rétention rénale par périurétérite. Libération externe de l'uretére. Assoc Fr Urol 1905;9:511–7.
[34] Vaglio A, Salvarani C, Buzio C. Retroperitoneal fibrosis. Lancet 2006;367:241–51.
[35] Uibu T, Oksa P, Auvinen A, Honkanen E, Metsarinne K, Saha H, Uitti J, Roto P. Asbestos exposure as a risk factor for retroperitoneal fibrosis. Lancet 2004;363:1422–6.
[36] Koep L, Zuidema GD. The clinical significance of retroperitoneal fibrosis. Surgery 1977;81:250–7.

Please cite this article in press as: Ishizaka N, et al. Multifocal fibrosclerosis and IgG4-related disease involving the cardiovascular system. J Cardiol (2012), doi:10.1016/j.jjcc.2011.10.005

[37] Chim CS, Liang R, Chan AC. Sclerosing malignant lymphoma mimicking idiopathic retroperitoneal fibrosis: importance of clonality study. Am J Med 2001;111:240–1.
[38] Sasaki S, Yasuda K, Takigami K, Yamauchi H, Shiiya N, Sakuma M. Inflammatory abdominal aortic aneurysms and atherosclerotic abdominal aortic aneurysms – comparisons of clinical features and long-term results. Jpn Circ J 1997;61:231–5.
[39] Yusuf K, Murat B, Unal A, Ulku K, Taylan K, Ozerdem O, Erdal Y, Tahsin Y. Inflammatory abdominal aortic aneurysm: predictors of long-term outcome in a case-control study. Surgery 2007;141:83–9.
[40] Serra RM, Engle JE, Jones RE, Schoolwerth AC. Perianeurysmal retroperitoneal fibrosis. An unusual cause of renal failure. Am J Med 1980;68:149–53.
[41] Ito H, Kaizaki Y, Noda Y, Fujii S, Yamamoto S. IgG4-related inflammatory abdominal aortic aneurysm associated with autoimmune pancreatitis. Pathol Int 2008;58:421–6.
[42] Kasashima S, Zen Y, Kawashima A, Endo M, Matsumoto Y, Kasashima F. A new clinicopathological entity of IgG4-related inflammatory abdominal aortic aneurysm. J Vasc Surg 2009;49:1264–71.
[43] Sakata N, Tashiro T, Uesugi N, Kawara T, Furuya K, Hirata Y, Iwasaki H, Kojima M. IgG4-positive plasma cells in inflammatory abdominal aortic aneurysm: the possibility of an aortic manifestation of IgG4-related sclerosing disease. Am J Surg Pathol 2008;32:553–9.
[44] Sakamoto A, Okamoto K, Ishizaka N, Tejima K, Hirata Y, Nagai R. 18F-fluorodeoxyglucose positron emission tomography in a case of retroperitoneal fibrosis. Int Heart J 2006;47:645–50.
[45] Sakamoto A, Nagai R, Saito K, Imai Y, Takahashi M, Hosoya Y, Takeda N, Fujihara M, Hirano K, Koike K, Enomoto Y, Kume H, Homma Y, Maeda D, Yamada H, et al. Idiopathic retroperitoneal fibrosis, inflammatory aortic aneurysm, and inflammatory pericarditis – retrospective analysis of 11 case histories. J Cardiol, doi:10.1016/j.jjcc.2011.07.014.
[46] Zen Y, Onodera M, Inoue D, Kitao A, Matsui O, Nohara T, Namiki M, Kasashima S, Kawashima A, Matsumoto Y, Katayanagi K, Murata T, Ishizawa S, Hosaka N, Kuriki K, et al. Retroperitoneal fibrosis: a clinicopathologic study with respect to immunoglobulin G4. Am J Surg Pathol 2009;33:1833–9.
[47] Crawford JL, Stowe CL, Safi HJ, Hallman CH, Crawford ES. Inflammatory aneurysms of the aorta. J Vasc Surg 1985;2:113–24.
[48] Okita Y, Takamoto S, Ando M, Kawashima Y, Matsuo H. A case report of inflammatory aneurysm of the thoracic aorta. J Vasc Surg 1995;21:999–1001.
[49] Roth M, Lemke P, Bohle RM, Klovekorn WP, Bauer EP. Inflammatory aneurysm of the ascending thoracic aorta. J Thorac Cardiovasc Surg 2002;123:822–4.
[50] Palmisano A, Vaglio A. Chronic periaortitis: a fibroinflammatory disorder. Best Pract Res Clin Rheumatol 2009;23:339–53.
[51] Bahler C, Hammoud Z, Sundaram C. Mediastinal fibrosis in a patient with idiopathic retroperitoneal fibrosis. Interact Cardiovasc Thorac Surg 2008;7:336–8.
[52] Gluhovschi G, Bozdog G, Miclaus G, Puscasiu T, Gluhovschi C, Bob F, Velciov S, Petrica L, Trandafirescu V, Gadalean F. Idiopathic retroperitoneal fibrosis with particular perirenal and intrarenal extension associated with left renal artery stenosis. The atheromatous periaortitis with retroperitoneal fibrosis suggests a pathogenic relationship between atherosclerosis and fibrosis? Wien Klin Wochenschr 2011;123:124–8.
[53] Ishida M, Hotta M, Kushima R, Asai T, Okabe H. IgG4-related inflammatory aneurysm of the aortic arch. Pathol Int 2009;59:269–73.
[54] Takahashi M, Shimizu T, Inajima T, Hosoya Y, Takeda N, Ishizaka N, Yamashita H, Hirata Y, Nagai R. A case of localized IgG4-related thoracic periarteritis and recurrent nerve palsy. Am J Med Sci 2011;341:166–9.
[55] Kasashima S, Zen Y, Kawashima A, Endo M, Matsumoto Y, Kasashima F, Ohtake H, Nakanuma Y. A clinicopathologic study of immunoglobulin G4-related sclerosing disease of the thoracic aorta. J Vasc Surg 2010;52:1587–95.
[56] Miyashita T, Yoshioka K, Shibata M, Kasamatsu Y, Nakamura T, Motoki M, Kato M, Hattori K, Shibata T, Yamagami K. Endovascular repair of sealed rupture of a thoracic inflammatory aneurysm that developed after corticosteroid therapy. Intern Med 2010;49:1221–4.
[57] Salvarani C, Calamia KT, Matteson EL, Hunder GG, Pipitone N, Miller DV, Warrington KJ. Vasculitis of the gastrointestinal tract in chronic periaortitis. Medicine (Baltimore) 2011;90:28–39.
[58] Scheel Jr PJ, Feeley N. Retroperitoneal fibrosis: the clinical, laboratory, and radiographic presentation. Medicine (Baltimore) 2009;88:202–7.
[59] Maturen KE, Sundaram B, Marder W, Swartz RD. Coronary artery involvement in idiopathic retroperitoneal fibrosis: computed tomographic findings. J Thorac Imaging 2011 [Epub ahead of print].
[60] Inoue D, Zen Y, Abo H, Gabata T, Demachi H, Yoshikawa J, Miyayama S, Nakanuma Y, Matsui O. Immunoglobulin G4-related periaortitis and periarteritis: CT findings in 17 patients. Radiology 2011;261:625–33.
[61] Sugimoto T, Morita Y, Isshiki K, Yamamoto T, Uzu T, Kashiwagi A, Horie M, Asai T. Constrictive pericarditis as an emerging manifestation of hyper-IgG4 disease. Int J Cardiol 2008;130: e100–1.
[62] Kawai S, Okada R. Interstitial cell infiltrate and myocardial fibrosis in dilated cardiomyopathy: a special type of cardiomegaly corresponding to sequelae of myocarditis. Heart Vessels 1990;5:230–6.
[63] Maehashi N, Yokota Y, Takarada A, Usuki S, Maeda S, Yoshida H, Sugiyama T, Fukuzaki H. The role of myocarditis and myocardial fibrosis in dilated cardiomyopathy. Analysis of 28 necropsy cases. Jpn Heart J 1991;32:1–15.
[64] Okura Y, Dec GW, Hare JM, Kodama M, Berry GJ, Tazelaar HD, Bailey KR, Cooper LT. A clinical and histopathologic comparison of cardiac sarcoidosis and idiopathic giant cell myocarditis. J Am Coll Cardiol 2003;41:322–9.
[65] Terasaki F, Kizawa H, Fujita S, Kanzaki Y, Kitaura Y, Ishizaka N. Assessment of serum IgG4 levels in cardiac and non-cardiac sarcoidosis. Hum Pathol, doi:10.1016/j.humpath.2011.07.002.
[66] Bennett DE. Primary mycotic aneurysms of the aorta. Report of case and review of the literature. Arch Surg 1967;94: 758–65.
[67] Kanemitsu S, Shimono T, Nakamura A, Yamamoto K, Wada H, Shimpo H. Molecular diagnosis of nonaneurysmal infectious aortitis. J Vasc Surg 2011;53:472–4.
[68] Takahashi N, Ghazale AH, Smyrk TC, Mandrekar JN, Chari ST. Possible association between IgG4-associated systemic disease with or without autoimmune pancreatitis and non-Hodgkin lymphoma. Pancreas 2009;38:523–6.
[69] Amiya E, Ishizaka N, Watanabe A, Endo Y, Itou R, Yoshida S, Nangaku M, Nagai R. Retroperitoneal fibrosis with periaortic and pericardial involvement. Circ J 2005;69:760–2.

Please cite this article in press as: Ishizaka N, et al. Multifocal fibrosclerosis and IgG4-related disease involving the cardiovascular system. J Cardiol (2012), doi:10.1016/j.jjcc.2011.10.005

Novel Insights from Clinical Experience

CARDIOLOGY

Cardiology 2011;120:22–26
DOI: 10.1159/000332996

Received: August 22, 2011
Accepted: August 23, 2011
Published online: November 16, 2011

Giant Tumorous Legions Surrounding the Right Coronary Artery Associated with Immunoglobulin-G4-Related Systemic Disease

Masayasu Ikutomi[a] Takayoshi Matsumura[a] Hiroshi Iwata[a] Go Nishimura[a]
Nobukazu Ishizaka[a] Yasunobu Hirata[a] Minoru Ono[b] Ryozo Nagai[a]

Departments of [a]Cardiovascular Medicine and [b]Cardiothoracic Surgery, The University of Tokyo, Tokyo, Japan

Established Facts

- A novel clinicopathological entity, immunoglobulin-G4-related systemic disease, can affect a wide variety of organs including the pancreas, bile duct, salivary glands and retroperitoneum.
- Further, immunoglobulin-G4-related systemic disease can be manifested as periarteritis, often as inflammatory abdominal aortic aneurysm.

Novel Insights

- Immunoglobulin-G4-related periarteritis can involve the coronary arteries.
- Immunoglobulin-G4-related systemic disease should be considered in any patient with abnormally increased wall thickness or ectatic lesions in the coronary arteries.

Key Words
Immunoglobulin-G4-related systemic disease · Coronary periarteritis · Autoimmune disease

Abstract
Immunoglobulin G4 (IgG4)-related systemic disease was first recognized as a clinicopathological entity about 10 years ago, and since then, it has attracted growing attention. It is an autoimmune disease which affects multiple organs including the pancreas, bile duct, salivary glands and retroperitoneum. Further, it was recently reported that it can be manifested as periarteritis, often as inflammatory abdominal aortic aneurysm. We describe the case of a 75-year-old man with autoimmune pancreatitis and parotitis who presented with angina. The serum concentration of IgG4 was significantly increased at 2,510 mg/dl. Coronary angiography showed multiple stenotic lesions and pronounced dilatation of the right coronary artery. Cardiac computed tomography disclosed increased wall thickness of the coronary arteries and focal tumorous lesions surrounding the right coronary artery. Treatment with steroids proved only marginally effective and he underwent surgical resection of the aneurysm and coronary artery bypass grafting. The diag-

KARGER

Fax +41 61 306 12 34
E-Mail karger@karger.ch
www.karger.com

0008–6312/11/1201–0022$38.00/0

Accessible online at:
www.karger.com/crd

Takayoshi Matsumura
Department of Cardiovascular Medicine
The University of Tokyo, 7-3-1 Hongo, Bunkyo-ku
Tokyo 113-8655 (Japan)
Tel. +81 3 3815 5411, ext. 33117, E-Mail tamatsum-tky@umin.ac.jp

nosis of IgG4-related systemic disease was confirmed by histological examination of the resected mass, which showed a massive infiltration of IgG4-positive plasma cells. This case emphasizes the importance of considering the diagnosis in any patient with abnormally increased wall thickness or ectatic lesions in the coronary arteries.

Introduction

Immunoglobulin G4 (IgG4)-related systemic disease is an autoimmune disorder in which IgG4-positive plasma cells infiltrate and expand in affected organs [1–6]. It was first recognized to involve the pancreas and is now known to involve diverse organs including not only the pancreas but also the bile duct, salivary glands, kidneys, lungs, retroperitoneum and aorta [7–10]. The spectrum of IgG4-related systemic disease is growing steadily, and it can be underdiagnosed simply due to a lack of awareness of this condition. We present a patient with IgG4-related coronary periarteritis in whom tumorous lesions surrounding the coronary arteries were demonstrated by cardiac computed tomography.

Case Report

A 75-year-old man was referred to our department for chest pain on exertion. He had a long history of diabetes mellitus, hyperlipidemia and hypertension, which had been adequately controlled with medications. At the age of 70 years, autoimmune pancreatitis was diagnosed by elevated serum IgG4 concentration and the findings on abdominal computed tomography and magnetic resonance imaging. It had been followed up without steroid therapy due to the lack of clinical symptoms. Also recently, he had bilateral parotitis with painful swelling of the parotid glands. On admission, he had severe xanthomas of the Achilles tendons and on the dorsum of the hands. Thus, a possible diagnosis of familial hypercholesterolemia was made, which was further supported by his family history of early atherosclerotic disease. Laboratory data showed an increase in erythrocyte sedimentation rate (112 mm/h). In addition, the serum concentration of total IgG was increased substantially (3,566 mg/dl, normal range 800–1,600), and the serum IgG4 level was dramatically elevated at 2,510 mg/dl (normal range 4.8–105).

Coronary angiography showed diffuse severe stenosis of the left anterior descending artery and focal stenosis in the proximal left circumflex artery (fig. 1a), and the right coronary artery was generally ectatic with pronounced dilatation of the distal segment (fig. 1b). Cardiac computed tomography disclosed increased wall thickness of the coronary arteries and, of note, two focal tumorous lesions surrounding the middle and distal portion of the right coronary artery were revealed (fig. 2a). The wall thickness of the aortic arch and the abdominal aorta was also increased (fig. 3). ^{18}F-fluorodeoxyglucose positron-emission tomography demonstrated intense uptake not only in the pancreas and the parotid glands, but also in the wall of the coronary arteries, suggesting active inflammation in these lesions (fig. 4).

The patient was clinically diagnosed with IgG4-related systemic disease and treated with prednisone 30 mg daily, followed by a taper of the daily dose by 5 mg per 2-week period. The swelling of the parotid glands resolved soon. The serum levels of total IgG and IgG4 decreased significantly to 1,266 and 676 mg/dl, respectively, and the diffuse pancreatic mass was reduced in size in 4 weeks. On the other hand, the thickened walls and tumorous tissues around the coronary arteries and the ectatic lesion of the right coronary artery were only marginally improved. The stenosis of the left cor-

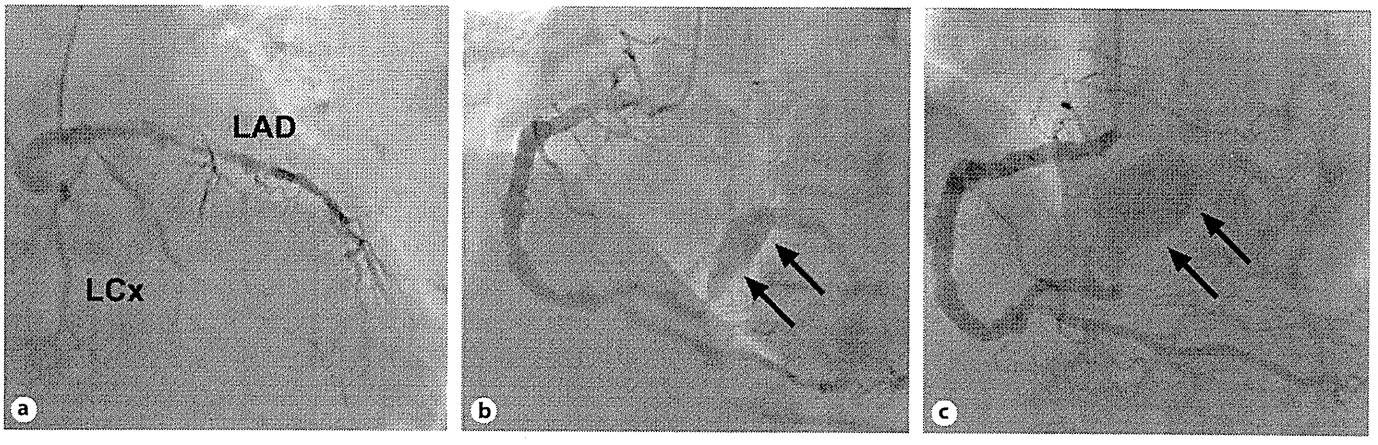

Fig. 1. Coronary angiography on first admission (**a**, **b**) and 4 months later (**c**). **a** Coronary angiography on first admission showing diffuse severe stenosis of the left anterior descending artery (LAD) and focal stenosis in the proximal left circumflex artery (LCx). **b** The right coronary artery was generally ectatic with pronounced dilatation of the distal segment (arrows). **c** Four months later, the ectatic lesion of the right coronary artery was further dilated (arrows).

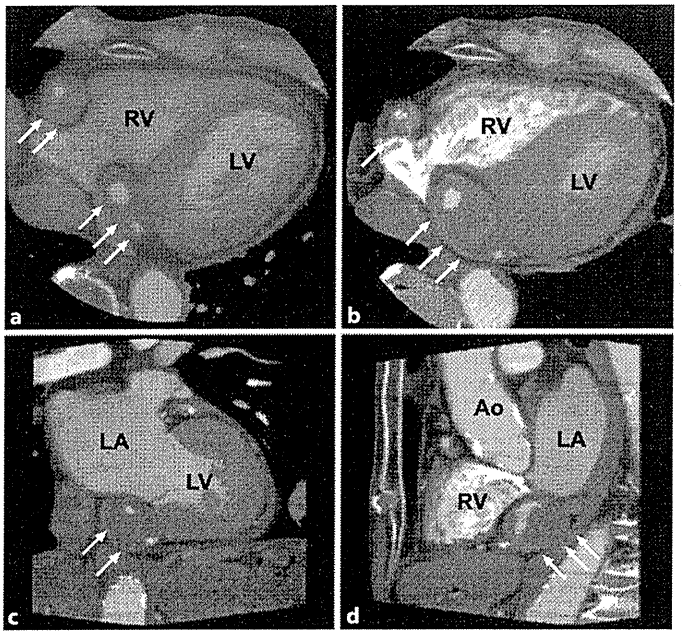

Fig. 2. Cardiac computed tomography on first admission (**a**) and 4 months later (**b–d**). RV = Right ventricle; LV = left ventricle; LA = left atrium; Ao = aorta. **a** Horizontal view of cardiac computed tomography on first admission demonstrating focal tumorous lesions surrounding the right coronary artery (arrows). **b–d** Four months later, the tumorous tissue in the distal portion (arrows) enlarged, as shown by horizontal (**b**), coronal (**c**) and sagittal view (**d**).

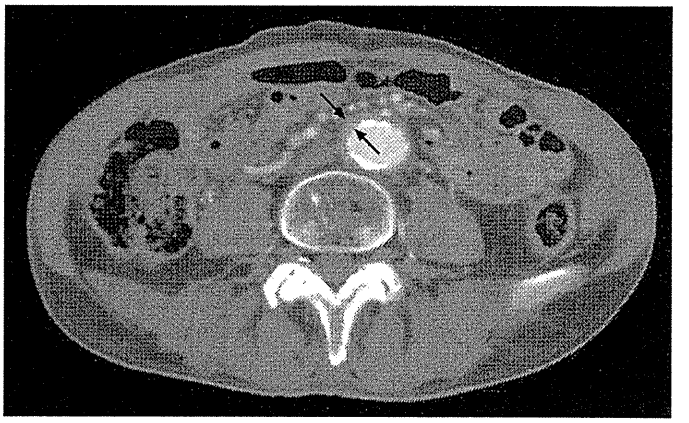

Fig. 3. Abdominal computed tomography showing the increased wall thickness of the abdominal aorta (arrows).

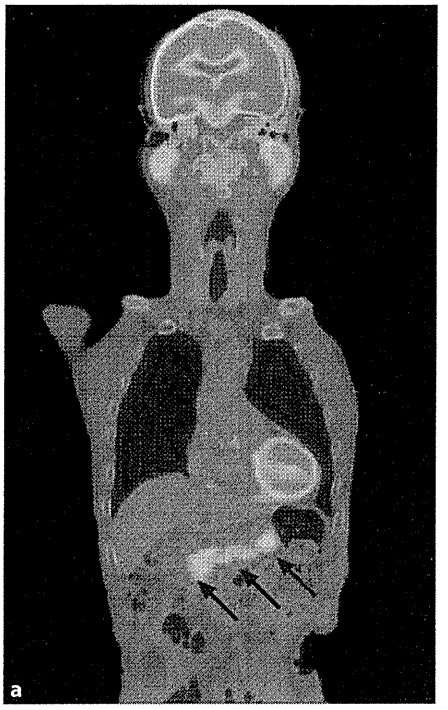

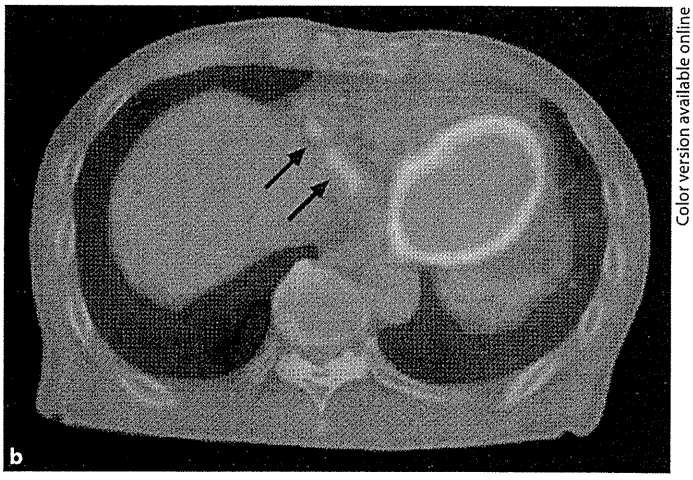

Color version available online

Fig. 4. ^{18}F-fluorodeoxyglucose positron-emission tomography demonstrating intense uptake not only in the pancreas (arrows) and the parotid glands (**a**), but also in the wall of the coronary arteries (arrows, **b**).

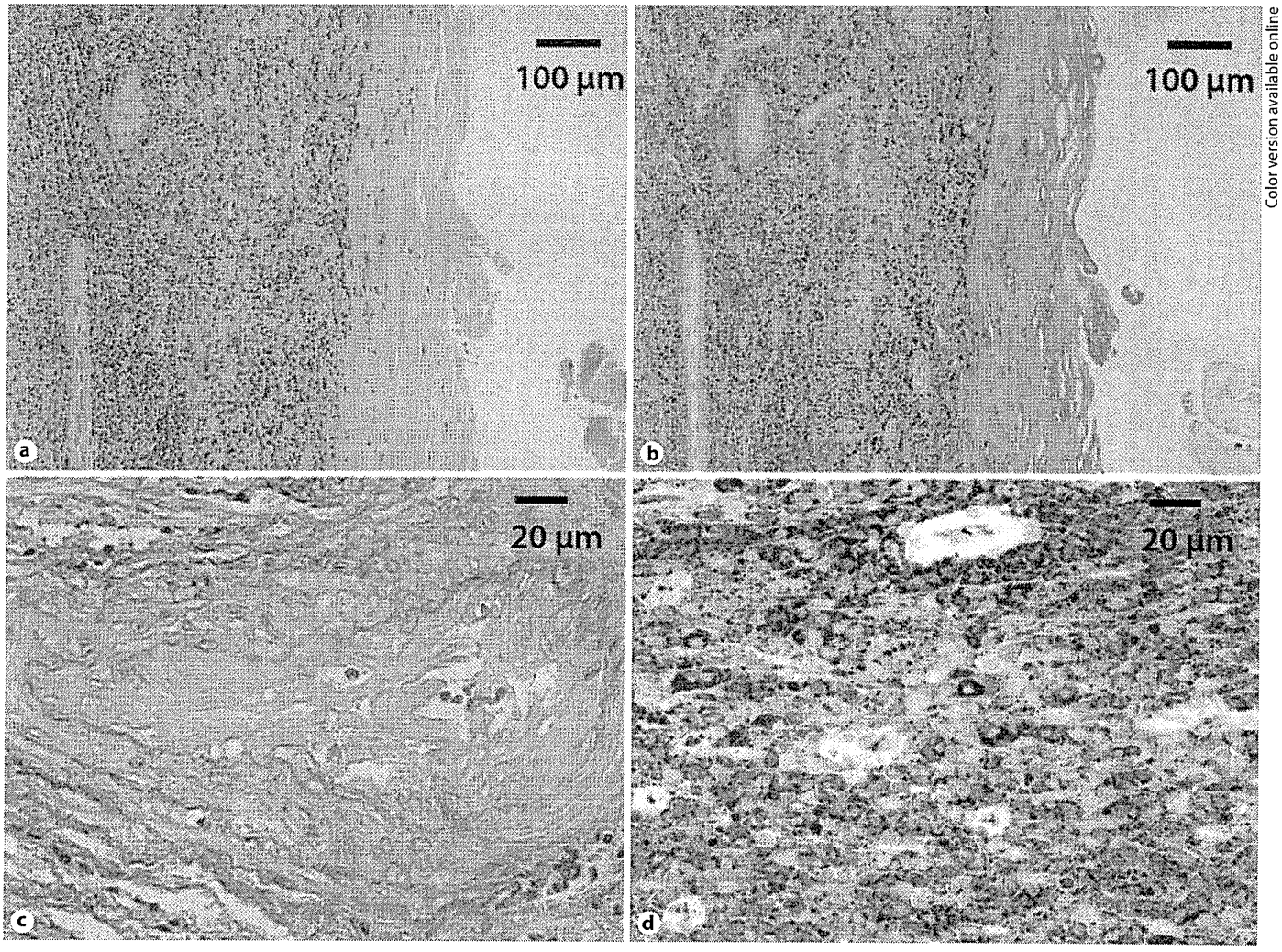

Color version available online

Fig. 5. Histological examination of the resected mass. **a**, **b** Massive lymphoplasmacytic infiltrate and fibrosis were shown mainly in the adventitia as demonstrated by hematoxylin-eosin staining (**a**) and elastin van Gieson staining (**b**). **c** The small vessels in the adventitia were hypertrophied and some of them were occluded by the thrombus. **d** Immunohistological analysis using an anti-IgG4 antibody revealing that a majority of infiltrated cells were IgG4-positive plasma cells.

onary artery still remained. We performed percutaneous coronary intervention with placement of two drug-eluting stents in the left anterior descending artery. He was discharged without symptoms, taking prednisone at a dose of 15 mg per day.

Four months later, follow-up angiography demonstrated that the ectatic lesion of the right coronary artery was further dilated (fig. 1c) and the surrounding tumorous tissue enlarged from 40 × 24 to 48 × 29 mm (fig. 2b–d). Considering the risk of rupture, the patient underwent surgical resection of the aneurysm and coronary artery bypass grafting by attaching a saphenous vein graft sequentially to the left circumflex artery and the distal portion of the right coronary artery. He was angina free with prednisone at a dose of 7.5 mg per day at the last follow-up visit 4 months after surgery.

Histological examination of the resected mass showed a prominent lymphoplasmacytic infiltrate and fibrosis predominantly in the adventitia, with destruction of normal structures of the intima and the media (fig. 5a, b). The small vessels in the adventitia were severely hypertrophied, and some of them were occluded by the thrombus (fig. 5c). Immunohistological analysis revealed that a majority of infiltrated cells were IgG4-positive plasma cells, thus confirming the diagnosis (fig. 5d).

Discussion

Since elevated serum IgG4 levels in patients with autoimmune pancreatitis were first reported in 2001 [3], there are rapidly emerging evidences that a novel clinico-

pathological entity, IgG4-related systemic disease, can affect multiple organs including the pancreas, bile duct, salivary glands and retroperitoneum [1–6]. Further, it is a recent topic of interest that IgG4-related systemic disease can be manifested as periarteritis, often as inflammatory abdominal aortic aneurysm [7–10]. A recent report described the first reported case of IgG4-related periarteritis presenting with a tumorous lesion of the right coronary artery [11]. The surgically resected mass showed the pathological features of diffuse lymphoplasmacytic infiltration and numerous IgG4-positive plasma cells. The radiological and histological findings are similar to those of our case. Thus, our case is considered to be the second reported case of IgG4-related periarteritis of the coronary arteries with severer manifestations. It is tempting to envision the possibility that concomitant familial hypercholesterolemia influenced these quite unusual radiological findings. Our patient was treated with steroids, and autoimmune pancreatitis and parotitis were ameliorated. However, on the other hand, the effect on periarteritis seemed to be limited, and surgical resection was required. While IgG4-related systemic disease often responds dramatically to corticosteroid therapy, there is no consensus on the optimal treatment of IgG4-related periarteritis, and further studies are needed.

The spectrum of IgG4-related systemic disease in the cardiovasculature is not fully understood, and IgG4-related periarteritis involving the coronary arteries may be underdiagnosed. IgG4-related systemic disease should be considered in any patient with abnormally increased wall thickness or ectatic lesions in the coronary arteries.

References

1 Stone JH, Caruso PA, Deshpande V: Case records of the Massachusetts General Hospital. Case 24-2009. A 26-year-old woman with painful swelling of the neck. N Engl J Med 2009;361:511–518.

2 Khosroshahi A, Stone JR, Pratt DS, Deshpande V, Stone JH: Painless jaundice with serial multi-organ dysfunction. Lancet 2009; 373:1494.

3 Hamano H, Kawa S, Horiuchi A, Unno H, Furuya N, Akamatsu T, Fukushima M, Nikaido T, Nakayama K, Usuda N, Kiyosawa K: High serum IgG4 concentrations in patients with sclerosing pancreatitis. N Engl J Med 2001;344:732–738.

4 Khosroshahi A, Stone JH: A clinical overview of IgG4-related systemic disease. Curr Opin Rheumatol 2011;23:57–66.

5 Raissian Y, Nasr SH, Larsen CP, Colvin RB, Smyrk TC, Takahashi N, Bhalodia A, Sohani AR, Zhang L, Chari S, Sethi S, Fidler ME, Cornell LD: Diagnosis of IgG4-related tubulointerstitial nephritis. J Am Soc Nephrol 2011;22:1343–1352.

6 Fervenza FC, Downer G, Beck LH Jr, Sethi S: IgG4-related tubulointerstitial nephritis with membranous nephropathy. Am J Kidney Dis 2011;58:320–324.

7 Kasashima S, Zen Y: IgG4-related inflammatory abdominal aortic aneurysm. Curr Opin Rheumatol 2011;23:18–23.

8 Stone JR: Aortitis, periaortitis, and retroperitoneal fibrosis, as manifestations of IgG4-related systemic disease. Curr Opin Rheumatol 2011;23:88–94.

9 Stone JH, Khosroshahi A, Hilgenberg A, Spooner A, Isselbacher EM, Stone JR: IgG4-related systemic disease and lymphoplasmacytic aortitis. Arthritis Rheum 2009;60: 3139–3145.

10 Kasashima S, Zen Y, Kawashima A, Endo M, Matsumoto Y, Kasashima F: A new clinicopathological entity of IgG4-related inflammatory abdominal aortic aneurysm. J Vasc Surg 2009;49:1264–1271.

11 Matsumoto Y, Kasashima S, Kawashima A, Sasaki H, Endo M, Kawakami K, Zen Y, Nakanuma Y: A case of multiple immunoglobulin G4-related periarteritis: a tumorous lesion of the coronary artery and abdominal aortic aneurysm. Hum Pathol 2008;39:975–980.

Evaluating Japanese Patients With the Marfan Syndrome Using High-Throughput Microarray-Based Mutational Analysis of Fibrillin-1 Gene

Naomi Ogawa, MD, PhD[a,c], Yasushi Imai, MD, PhD[a,c], Yuji Takahashi, MD, PhD[d,e], Kan Nawata, MD, PhD[b], Kazuo Hara, MD, PhD[c,g], Hiroshi Nishimura, MD, PhD[a], Masayoshi Kato, MD, PhD[a], Norifumi Takeda, MD, PhD[a], Takahide Kohro, MD, PhD[c,h], Hiroyuki Morita, MD, PhD[h], Tsuyoshi Taketani, MD, PhD[b], Tetsuro Morota, MD, PhD[b], Tsutomu Yamazaki, MD, PhD[c,f], Jun Goto, MD, PhD[d,e], Shoji Tsuji, MD, PhD[d,e], Shinichi Takamoto, MD, PhD[b], Ryozo Nagai, MD, PhD[a,c], and Yasunobu Hirata, MD, PhD[a,*]

Marfan syndrome (MS) is an inherited connective tissue disorder, and detailed evaluations of multiple organ systems are required for its diagnosis. Genetic testing of the disease-causing fibrillin-1 gene (FBN1) is also important in this diagnostic scheme. The aim of this study was to define the clinical characteristics of Japanese patients with MS and enable the efficient and accurate diagnosis of MS with mutational analysis using a high-throughput microarray-based resequencing system. Fifty-three Japanese probands were recruited, and their clinical characteristics were evaluated using the Ghent criteria. For mutational analysis, an oligonucleotide microarray was designed to interrogate FBN1, and the entire exon and exon-intron boundaries of FBN1 were sequenced. Clinical evaluation revealed more pulmonary phenotypes and fewer skeletal phenotypes in Japanese patients with MS compared to Caucasians. The microarray-based resequencing system detected 35 kinds of mutations, including 23 new mutations. The mutation detection rate for patients who fulfilled the Ghent criteria reached 71%. Of note, splicing mutations accounted for 19% of all mutations, which is more than previously reported. In conclusion, this comprehensive approach successfully detected clinical phenotypes of Japanese patients with MS and demonstrated the usefulness and feasibility of this microarray-based high-throughput resequencing system for mutational analysis of MS. © 2011 Elsevier Inc. All rights reserved. **(Am J Cardiol 2011;108:1801–1807)**

The Marfan syndrome (MS) is an inherited connective tissue disorder with an autosomal dominant inheritance, primarily involving the skeletal, ocular, and cardiovascular systems, caused by mutations in fibrillin-1 gene (FBN1).[1] Diagnosis of the MS has been made using the Ghent criteria[2] on the basis of data from European and American populations, but the Ghent criteria may not be completely suitable for the Japanese population.[3] Therefore, epidemiologic and genetic surveys in the Japanese population are mandatory to establish more Japanese-specific (or Asian-specific) diagnostic criteria for the MS. The Ghent criteria were recently further revised.[4] More weight is now given to FBN1 testing, and a diagnosis can be made if a patient has the FBN1 mutation plus either an aortic phenotype or ectopia lentis. These new criteria are much simpler than the original criteria. Thus, genetic testing of MS is becoming more important. FBN1 spans a 230-kb genomic region and contains 65 exons. More than 1,000 reported mutations are spread throughout the gene and are mostly unique in each affected family.[5,6] Classic genetic analysis methods such as direct sequencing are very time consuming. Thus, the introduction of a more efficient genetic analysis tool is needed. Custom-designed resequencing microarrays enable the analysis of multiple genes spanning 30 to 300 kb on a single array. The microarray identifies individual nucleotides by comparative, high-fidelity hybridization using oligonucleotide probes[7–9] (Figure 1). In the present study, we comprehensively evaluated the clinical characteristics of Japanese patients with suspected MS and also conducted mutational analysis of these patients by adopting a high-throughput genetic diagnosing system to achieve more efficient and accurate diagnoses.

Methods

Fifty-three consecutive probands suspected of having MS who visited the MS clinic at our hospital were enrolled. All patients were assessed using the original Ghent criteria.[2,10] This study was conducted according to the Declara-

[a]Departments of Cardiovascular Medicine, [b]Cardiothoracic Surgery, [c]Clinical and Genetic Informatics, [d]Neurology, [e]Clinical Genomics, [f]Clinical Epidemiology and Systems, [g]Metabolic Diseases, and [h]Translational Research for Healthcare and Clinical Science, Graduate School of Medicine, University of Tokyo, Tokyo, Japan. Manuscript received April 26, 2011; revised manuscript received and accepted July 15, 2011.

This work was supported by Health Labor Science's Research Grants from the Japanese Ministry of Health, Labor, and Welfare (Grant 10103493 to Dr. Hirata), the Human Resources Development Program of the Japanese Ministry of Education, Culture, Sports and Technology and JSPS through its FIRST Program (Drs. Yamazaki and Nagai).

*Corresponding author: Tel: 81-3815-5411; fax: 81-3-5800-9845.
E-mail address: hirata-2im@h.u-tokyo.ac.jp (Y. Hirata).

0002-9149/11/$ – see front matter © 2011 Elsevier Inc. All rights reserved.
doi:10.1016/j.amjcard.2011.07.053

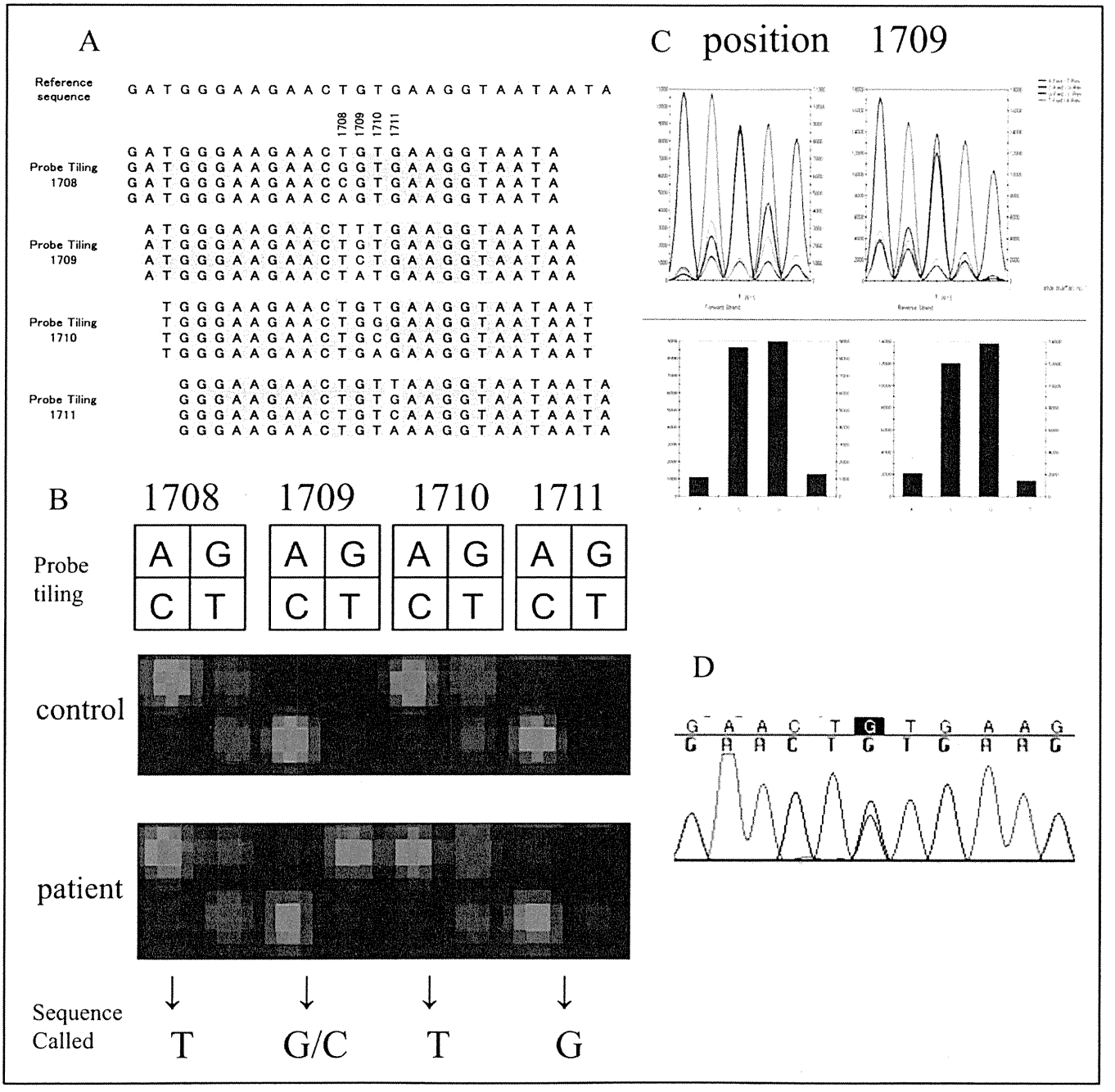

Figure 1. Representative example of mutational analysis using the present microarray-based resequencing system. *(A)* The microarray identifies individual nucleotides by comparative, high-fidelity hybridization using oligonucleotide probes that are synthesized in situ by photolithography and solid-phase DNA synthesis. For each base position, 8 unique 25-mer probes (4 oligonucleotide probes for each strand) are tiled on the array, and each 25-mer probe is varied at the central position to incorporate each possible nucleotide (A, G, C, or T), allowing the detection of all possible nucleotide substitutions. *(B)* Scan images of the probes around the nucleotide position 1709. In patients with the FBN1 c.1709G>C mutation, high signal intensities can be observed in probe G and C at nucleotide 1709 compared to control. *(C,D)* Signal intensity data at nucleotide position 1709. The intensity data for each base position can be also displayed as traces and bar graphs. The missense mutation (c.1709G>C) was successfully detected *(C)* and was verified by direct sequencing *(D)*.

tion of Helsinki and was approved by the institutional ethics committee. Written informed consent was obtained after providing a detailed explanation of the study. Genomic deoxyribonucleic acid (DNA) was extracted from buffy coat using a Genomix DNA extraction kit (Talent, Trieste, Italy). For amplification of the 65 exons of FBN1, polymerase chain reaction (PCR) primers were designed by referring to previous reports.[11–13] After performing the PCRs according to the standard protocol, the PCR products were subjected to hybridization on the microarray.

The resequencing microarray was designed on the basis of the reference sequences from the Ensembl database. Because highly homologous sequences lead to cross-hybridization, FBN1 was checked for possible repetitive sequences using RepeatMasker software (http://repeatmasker.org/chi-bin/webrepeatmasker). No repetitive elements were

Table 1
Background of participants who underwent genetic analysis (n = 53)

Variable	Total (n = 53)	Ghent-Positive Patients (n = 45)
Age (years)	33.1 ± 9.8	33.1 ± 10.4
Men	35/53 (66%)	30/45 (67%)
Ghent positive	45/53 (85%)	45/45 (100%)
Skeletal major criteria	12/49 (25%)	12/41 (29%)
Skeletal minor criteria	19/49 (39%)	17/41 (42%)
Ectopia lentis	25/53 (47%)	25/45 (56%)
Cardiovascular major criteria	48/53 (91%)	44/45 (98%)
Cardiovascular minor criteria	36/48 (75%)	32/41 (78%)
Pulmonary	22/49 (45%)	19/42 (45%)
Skin	26/49 (53%)	23/42 (55%)
Dural ectasia	34/47 (72%)	33/40 (83%)
Family history of MS	31/55 (56%)	28/45 (62%)

Data are expressed as mean ± SD or as number (percentage).

observed. The microarray contained sense and antisense sequences for the 65 exons of FBN1 and ≥12 flanking base pairs of the splice junctions. The PCR product was fragmented, end-labeled with biotin, and hybridized to the array. Washing and staining with streptavidin-phycoerythrin were performed on automated fluidic stations according to the manufacturer's protocol (Affymetrix, Santa Clara, California). Hybridization signals were read by a high-resolution laser scanner, and the data collection and interpretation were carried out using GeneChip Operating Software and GeneChip Sequence Analysis Software (Affymetrix), respectively.

Candidate nucleotide substitutions detected by the microarray-based resequencing system were subsequently validated by fluorescent dideoxy DNA sequencing using BigDye terminator version 3.1 on an ABI PRISM 3100xl genetic analyzer (Applied Biosystems, Foster City, California).

Some patients underwent cardiovascular surgery, and written informed consent for research use of surgical specimens was obtained from each patient. Total ribonucleic acid (RNA) was extracted using an RNeasy Fibrous Tissue Mini Kit (Qiagen, Venlo, The Netherlands). For patients whose aortic tissues were not available, total RNA was extracted from blood using a QIAamp RNA Blood Mini Kit (Qiagen). The RNA was converted to complementary DNA using SuperScript III First-Strand Synthesis SuperMix (Invitrogen, Carlsbad, California). PCR analyses were performed with specific primers designed for the target regions. PCR samples or subcloned plasmids after TA cloning of PCR products using a TOPO-TA vector (Invitrogen) were subjected to fluorescent dideoxy DNA sequencing.

DNA from patients whose mutations were not found by the aforementioned methods was screened by multiplex ligation-dependent probe amplification using a SALSA MLPA kit P065/P066 (MRC-Holland, Amsterdam, The Netherlands)[14] for large deletions and duplications.

All quantitative data are expressed as mean ± SD. Statistical comparisons of distributions between groups were made using the chi-square test. Significance was taken as $p < 0.05$.

Table 2
Detailed clinical findings of Ghent-positive patients (n = 45)

Criterion	n (%)
Skeletal major criteria	
Pectus carinatum	9/42 (21%)
Pectus excavatum, requiring surgery	7/44 (16%)
Arm span/height ratio >1.05	8/41 (20%)
Wrist and thumb signs	32/43 (74%)
Scoliosis of >20% or spondylolisthesis	21/44 (48%)
Reduced extension at the elbows (<170°)	2/41 (5%)
Medial displacement of medial malleolus, causing pes planus	16/41 (39%)
Protrusio acetabuli	8/39 (21%)
Skeletal minor criteria	
Pectus excavatum of moderate severity	10/44 (23%)
Joint hypermobility	7/41 (17%)
Highly arched palate with crowding of teeth	31/40 (78%)
Facial appearance	15/40 (38%)
Cardiovascular major criteria	
Dilatation/dissection of the ascending aorta	44/45 (98%)
Cardiovascular minor criteria	
Mitral valve prolapse	23/42 (55%)
Dilatation of main pulmonary artery	9/20 (45%)
Calcification of mitral annulus	0/34 (0%)
Dilatation/dissection of descending thoracic/abdominal aorta	12/43 (28%)
Pulmonary minor criteria	
Spontaneous pneumothorax	13/43 (30%)
Apical blebs	15/44 (34%)
Skin minor criteria	
Striae atrophicae	24/42 (57%)
Recurrent or incisional herniae	0/41 (0%)

Results

Of the 53 probands enrolled, 45 were diagnosed with MS according to the original Ghent criteria. Because our Marfan clinic offers cardiac surgery and some patients were referred for aortic surgery from other hospitals, most of the patients had aortic phenotypes (Table 1). Dural ectasia and ectopia lentis were common findings, and positive family histories were seen in about half of the probands. We confirmed a lower frequency for some of the skeletal manifestations in Japanese patients with MS compared to that reported in a Western database, such as an arm span/height ratio >1.05 (20% in our study vs 55% in Western populations) and reduced extension at the elbows (<170°) (5% vs 15%), findings that were similar to the report of Akutsu et al[3,6] (Table 2). However, the frequency of major skeletal criteria (29%) was higher than a previous Japanese report (15%), which is partially due to a lack of evaluation of protrusio acetabuli in the earlier study. We found a higher frequency of spontaneous pneumothorax (30% vs 7%) in our Japanese population compared to a previous study conducted in Western patients. Calcification of the mitral annulus and frequency of dilatation of the main pulmonary artery were rarely reported. Actually, mitral annular calcification was not detected at all. However, pulmonary artery dilatation was relatively frequent (45% [9 of 20]) in our study, after excluding those patients whose main pulmonary artery diameters were difficult to evaluate.

Table 3
Mutations found in this study

Exon	Complementary DNA	Protein
Missense mutations		
4	c.386G>A	p.Cys 129 Tyr
13	c.1709G>C*	p.Cys 570 Ser
14	c.1786T>G*	p.Cys 596 Gly
15	c.1911T>G*	p.Cys 637 Trp
18	c.2171T>G*	p.Ile 724 Arg
18	c.2201G>T	p.Cys 734 Phe
21	c.2638G>A	p.Gly 880 Ser
24	c.3043G>A	p.Ala 1015 Thr
26	c.3263A>G*	p.Asn 1088 Ser
28	c.3503A>G	p.Asn 1168 Ser
34	c.4280A>G*	p.Tyr 1427 Cys
43	c.5371T>C*	p.Cys 1791 Arg
47	c.5873G>A*	p.Cys 1958 Tyr
50	c.6296G>T	p.Cys 2099 Phe
53	c.6518G>A*	p.Gly 2173 Ser
57	c.7015T>G*	p.Cys 2339 Gly
60	c.7466G>A*	p.Cys 2489 Tyr
62	c.7754T>C	p.Ile 2585 Thr (2 probands)
Nonsense mutations		
8	c.945T>A*	p.Cys 315 X
12	c.1585C>T	p.Arg 529 X
29	c.3603C>A*	p.Cys 1201 X
37	c.4709G>A*	p.Trp 1570 X
38	c.4777G>T*	p.Glu 1593 X
38	c.4786C>T	p.Arg 1596 X
54	c.6658C>T	p.Arg 2220 X
58	c.7240C>T	p.Arg 2414 X
65	c.8521G>T*	p.Glu 2841 X
Splicing mutations		
11–12	c.IVS11+5G>A	p.Cys474Tyr Glu475_Asp490del
15–16	c.IVS15-3T>G*	
16–17	c.IVS16+3A>C*	
18–19	c.IVS18+1G>C*	
34–35	c.IVS34-1G>A*	p.Asp1446ValfsX21
40–41	c.IVS40+1G>A*	
52–53	c.6453C>T*	p.Cys2151Tyr, Glu2152_Asp2166del
56–57	c.IVS56+5G>A*	
Deletion mutations		
54	c.6665delT*	p.Val2222GlyFsX69
54	c.6703-6704delGG*	p.Gly2235IlefsX7
55	c.6837delG*	p.Tyr2280IlefsX10
57	c. 7071_7079delCGTCACCAA*	p.Val2358SerfsX511
65	c. 8532_8delTACAACT*	p.Thr2785X
3	Exon 3 deletion*	

* Newly found mutation.

In our mutational analysis, the base call rate of this system for FBN1 was >96% when examining 5 representative cases, and resequencing as many as 12,688 bp per patient was easily accomplished in 3 working days, demonstrating the high fidelity and high throughput of this system.

In the 53 probands, 35 kinds of FBN1 mutations were found in 36 probands using this system (Table 3). There were 18 missense and 9 nonsense mutations. Eight other mutations located near the exon-intron boundaries were thought to alter the splicing patterns. Supplemental direct sequencing in probands with no mutation detected by the microarray-based method revealed 5 deletion mutations in FBN1 (Table 3). Furthermore, multiplex ligation-dependent probe amplification assay revealed a large deletion mutation (exon 3) in 1 proband. Finally, novel mutations were found in 23 probands using microarray and in 29 probands in total. All possible mutations found by the microarray-based resequencing system were verified by direct sequencing, and thus the microarray detected point mutations with 100% accuracy. A representative example of genetic analysis using the microarray-based resequencing system is shown in Figure 1. Of 18 missense mutations, 11 were either affecting or creating cysteine residues. For other novel missense mutations, none of the mutations were found in ≥200 ethnically matched control subjects. The mutation detection rate

Table 4
Number of mutations detected

Mutation Detection Method	Total (n = 53)	Ghent Positive (n = 45)	Other (n = 8)
Microarray	36 (68%)	32 (71%)	4 (50%)
Direct sequencing	5 (9%)	5 (11%)	0
Multiplex ligation-dependent probe amplification	1 (2%)	1 (2%)	0
Total of all 3 modalities	42 (79%)	38 (84%)	4 (50%)

of the microarray-based resequencing system for the Ghent-positive patients was 71%. The overall mutation detection rate after additional analysis by fluorescent dideoxy DNA sequencing and multiplex ligation-dependent probe amplification reached 84% (Table 4).

Eight possible splicing mutations were identified, and these mutations constituted 19% of all mutations, which was more than the 11% currently reported in the UMD-FBN1 mutation database.[5] One patient and his 2 relatives with MS had the same silent mutation in FBN1 exon 52 (c.6453C>T, p.Cys2151Cys; Figure 2). Therefore, we re-sequenced complementary DNA from his aortic tissue and verified an alternation of the splicing pattern between FBN1 exon 52 and 53. The C at nucleotide position 6453 of FBN1 complementary DNA was substituted with a T, which resulted in the creation of a new splicing donor site, causing abnormal shorter messenger RNA. Another patient had a mutation at the fifth nucleotide of the beginning of intron 11 (c.IVS11+5G>A), although it is well known that the first 2 nucleotides at the beginning of the intron are very important as a splice donor site. We found by sequencing the complementary DNA that the latent splice donor site within exon 11 was activated and created the frame-shift mutation (Figure 2).

Six additional mutations possibly causing a splicing aberration were also found (Table 3). Although aortic tissue was unavailable for these patients, splicing aberrations were successfully confirmed in 2 whose complementary DNA was clinically available by resequencing FBN1 complementary DNA obtained from peripheral blood (Figure 2).

In published research, it has been suggested that mutations causing the in-frame loss or gain of the central coding sequence through deletions, insertions, or splicing errors are thought to be associated with more severe disease phenotypes. In contrast, nonsense mutations that result in rapid degradation of mutant transcripts are reported to be potentially associated with milder conditions. However, we could not find any associations between mutation types and clinical severity in our study subjects. A higher incidence of ectopia lentis in patients who carried a missense mutation involving a cysteine substitution or splicing mutation has been reported.[15] However, these correlations were not observed in our study. Among 4 patients who had mutations located between FBN1 exons 24 and 32, the so-called "neonatal region," none had the neonatal or early-onset form of MS.

Discussion

The Ghent criteria for MS diagnosis are based on data obtained mainly from European and American populations. Our clinical evaluations revealed that there were more pulmonary phenotypes and fewer skeletal phenotypes in Japanese patients with MS compared to Western patients. Therefore, the criteria for systemic and orthopedic features in the Ghent nosology may not be entirely suitable for application to Japanese and perhaps other Asian populations. Further epidemiologic and genetic studies in the Japanese population should be conducted to establish Asian- or Japanese-specific diagnostic criteria for MS.

The present microarray-based resequencing system is an efficient method for rapid and affordable mutation analysis of heterogenous disorders such as MS. The mutation detection rate is influenced by the accuracy of the clinical diagnosis of MS, the type of mutation, and the ability of the testing method. It ranged from 55% to 91% in previous reports.[11,16-18] The mutation detection rate of our system was concordant with previous reports. Its greatest advantages are high throughput and digitalized sequencing data. The digitally retrieved sequencing data are easily computable and can be displayed in various ways. In most of the cases, we could identify the mutations within a few minutes of data collection. Several other causative genes, such as transforming growth factor receptor types 1 and 2 (TGFBR1 and TGFBR2),[19] smooth muscle α-actin (ACTA2),[20] myosin heavy chain 11 (MYH11),[21] and SMAD3,[22] have been identified for syndromic or nonsyndromic aortic aneurysms and dissection. Such additional candidate genes can also be included on the same array because 1 array can resequence up to 300 kb.

Our system can detect point mutations with 100% accuracy and thus is a reliable first screening method for detecting single nucleotide substitutions. In contrast, it is difficult to detect heterozygous deletion or insertion mutations, because an abnormal allele containing a deletion or an insertion mutation is difficult to hybridize to probes. For patients with MS with no mutation detected by the microarray system, conventional direct sequencing and multiplex ligation-dependent probe amplification was helpful for searching for possible deletion or insertion mutations. Because there is a certain number of patients with MS without mutations in FBN1,[12,19] the 7 probands without any mutations may have possessed mutations in undiscovered disease-causing genes.

Eight splicing mutations that accounted for 19% of all the mutations were found. Because this type of mutation represented a greater proportion than that of previous reports, every exon-intron boundary should be resequenced. It is also advisable to obtain messenger RNA in addition to DNA for analyzing the splicing pattern. We successfully demonstrated altered splicing patterns using FBN1 messenger RNA extracted from peripheral leukocytes. Thus, we also recommend the extraction of RNA as well as genomic DNA from peripheral blood, if a surgically retrieved specimen is not available.

We also assessed patients using the recently published revised Ghent criteria. Forty-two of the 45 original Ghent-positive patients were also diagnosed with MS using the revised criteria. One patient, who was positive according to the original Ghent criteria, did not satisfy the revised criteria and was diagnosed with ectopia lentis syndrome. Two patients (aged 20 and 30 years) failed to meet the revised Ghent criteria because their z scores of aortic diameter were not

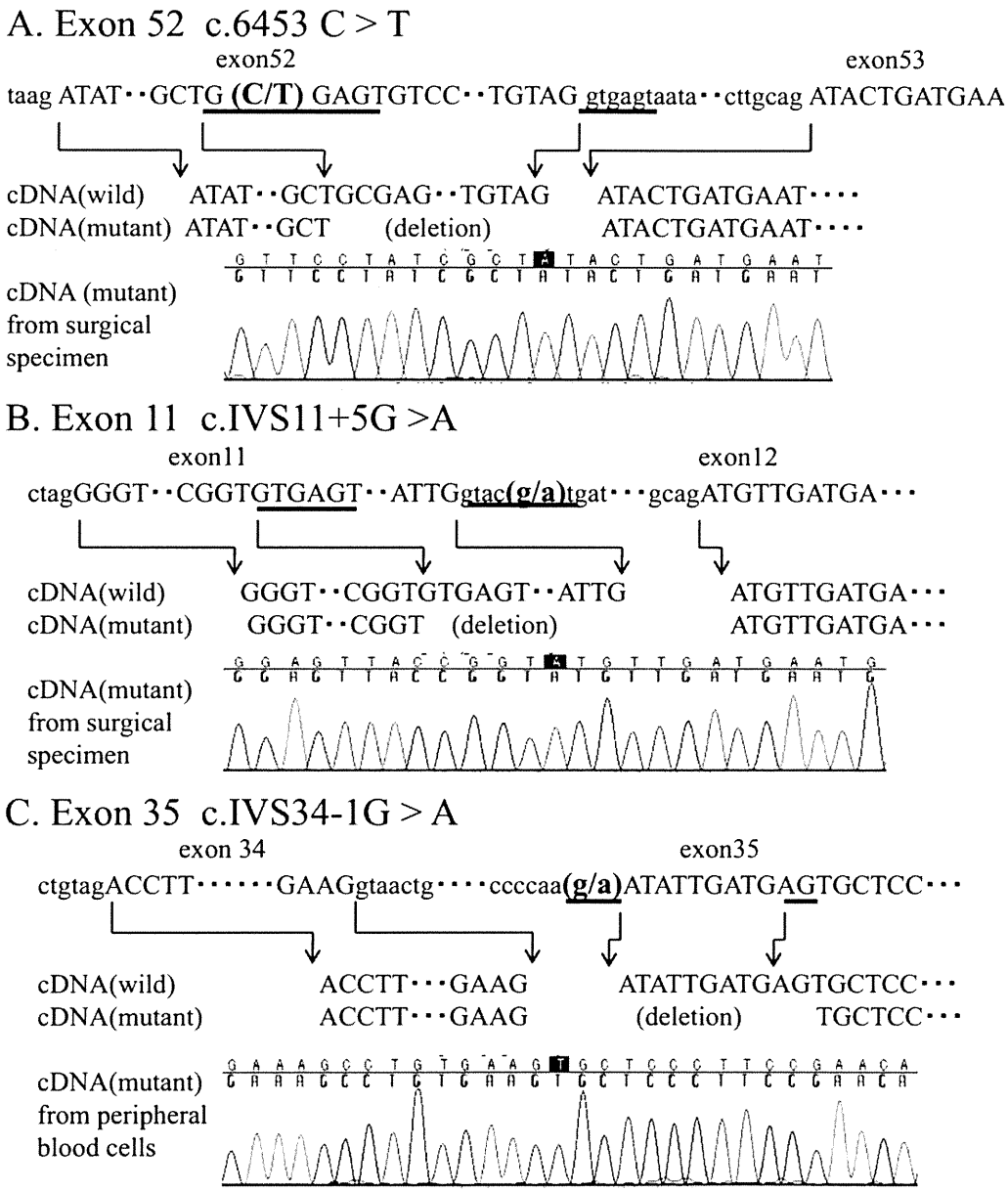

Figure 2. Representative splicing mutations in our study. *(A)* C-to-T substitution at nucleotide position 6453 produced a 6-nucleic acid sequence (c.6452-6457) *(underlined)* identical to that of IVS52+1 to +6 (gtgagt) *(underlined)*, and this was recognized as the splicing donor site. The following nucleotides of exon 52 from this point were deleted in the mutant allele. *(B)* The fifth nucleotide at the beginning of intron 11 was substituted from G to A (c.IVS11+5G>A). Resequencing of complementary DNA revealed that the latent splice donor site within exon 11 *(underlined)* was activated and became a new splice donor site and created the frame-shift mutation. *(C)* The last nucleotide of intron 34 was substituted from G to A (c.IVS34-1G>A). Resequencing FBN1 complementary DNA obtained from the peripheral blood demonstrated the splicing aberration, resulting in the deletion of 11 nucleotides of exon 35.

satisfactory, although their aortas dilated gradually later on. One patient met the revised Ghent criteria after genetic analysis of FBN1. Although further studies are warranted to clarify the properties and usefulness of the novel Ghent criteria, genetic testing is more important, although it is not mandatory. In such a setting, a high-throughput resequencing method such as the present microarray-based resequencing system can be a powerful tool for making an accurate diagnosis of MS.

Acknowledgments: We would like to express our sincere gratitude to the patients and their families for agreeing to participate in this work and to all the doctors in the MS clinic for their valuable advice. We also thank Wu Zhenghong, Eri Kasukawa, Ryohei Kataoka, Keiko Hori, Yumiko Fujimaki, and Takako Kawamura for their excellent technical assistance.

1. Dietz HC, Pyeritz RE. Mutations in the human gene for fibrillin-1 (FBN1) in the Marfan syndrome and related disorders. *Hum Mol Genet* 1995;4:1799-1809.
2. De Paepe A, Devereux RB, Dietz HC, Hennekam RC, Pyeritz RE. Revised diagnostic criteria for the Marfan syndrome. *Am J Med Genet* 1996;62:417-426.

3. Akutsu K, Morisaki H, Takeshita S, Ogino H, Higashi M, Okajima T, Yoshimuta T, Tsutsumi Y, Nonogi H, Morisaki T. Characteristics in phenotypic manifestations of genetically proved Marfan syndrome in a Japanese population. *Am J Cardiol* 2009;103:1146–1148.
4. Loeys BL, Dietz HC, Braverman AC, Callewaert BL, De Backer J, Devereux RB, Hilhorst-Hofstee Y, Jondeau G, Faivre L, Milewicz DM, Pyeritz RE, Sponseller PD, Wordsworth P, De Paepe AM. The revised Ghent nosology for the Marfan syndrome. *J Med Genet* 2010; 47:476–485.
5. Collod-Béroud G, Le Bourdelles S, Ades L, Ala-Kokko L, Booms P, Boxer M, Child A, Comeglio P, De Paepe A, Hyland JC, Holman K, Kaitila I, Loeys B, Matyas G, Nuytinck L, Peltonen L, Rantamaki T, Robinson P, Steinmann B, Junien C, Béroud C, Boileau C. Update of the UMD-FBN1 mutation database and creation of an FBN1 polymorphism database. *Hum Mutat* 2003;22:199–208.
6. Faivre L, Collod-Beroud G, Loeys BL, Child A, Binquet C, Gautier E, Callewaert B, Arbustini E, Mayer K, Arslan-Kirchner M, Kiotsekoglou A, Comeglio P, Marziliano N, Dietz HC, Halliday D, Beroud C, Bonithon-Kopp C, Claustres M, Muti C, Plauchu H, Robinson PN, Adès LC, Biggin A, Benetts B, Brett M, Holman KJ, De Backer J, Coucke P, Francke U, De Paepe A, Jondeau G, Boileau C. Effect of mutation type and location on clinical outcome in 1,013 probands with Marfan syndrome or related phenotypes and FBN1 mutations: an international study. *Am J Hum Genet* 2007;81:454–466.
7. Cutler DJ, Zwick ME, Carrasquillo MM, Yohn CT, Tobin KP, Kashuk C, Mathews DJ, Shah NA, Eichler EE, Warrington JA, Chakravarti A. High-throughput variation detection and genotyping using microarrays. *Genome Res* 2001;11:1913–1925.
8. Warrington JA, Shah NA, Chen X, Janis M, Liu C, Kondapalli S, Reyes V, Savage MP, Zhang Z, Watts R, DeGuzman M, Berno A, Snyder J, Baid J. New developments in high throughput resequencing and variation detection using high-density microarrays. *Hum Mutat* 2002;19:402–409.
9. Takahashi Y, Seki N, Ishiura H, Mitsui J, Matsukawa T, Kishino A, Onodera O, Aoki M, Shimozawa N, Murayama S, Itoyama Y, Suzuki Y, Sobue G, Nishizawa M, Goto J, Tsuji S. Development of a high-throughput microarray-based resequencing system for neurological disorders and its application to molecular genetics of amyotrophic lateral sclerosis. *Arch Neurol* 2008;65:1326–1332.
10. Roman MJ, Devereux RB, Kramer-Fox R, O'Loughlin J. Two-dimensional echocardiographic aortic root dimensions in normal children and adults. *Am J Cardiol* 1989;64:507–512.
11. Sakai H, Visser R, Ikegawa S, Ito E, Numabe H, Watanabe Y, Mikami H, Kondoh T, Kitoh H, Sugiyama R, Okamoto N, Ogata T, Fodde R, Mizuno S, Takamura K, Egashira M, Sasaki N, Watanabe S, Nishimaki S, Takada F, Nagai T, Okada Y, Aoka Y, Yasuda K, Iwasa M, Kogaki S, Harada N, Mizuguchi T, Matsumoto N. Comprehensive genetic analysis of relevant four genes in 49 patients with Marfan syndrome or Marfan-related phenotypes. *Am J Med Genet* 2006;140: 1719–1725.
12. Mizuguchi T, Collod-Beroud G, Akiyama T, Abifadel M, Harada N, Morisaki T, Allard D, Varret M, Claustres M, Morisaki H, Ihara M, Kinoshita A, Yoshiura K, Junien C, Kajii T, Jondeau G, Ohta T, Kishino T, Furukawa Y, Nakamura Y, Niikawa N, Boileau C, Matsumoto N. Heterozygous TGFBR2 mutations in Marfan syndrome. *Nat Genet* 2004;36:855–860.
13. Nijbroek G, Sood S, McIntosh I, Francomano CA, Bull E, Pereira L, Ramirez F, Pyeritz RE, Dietz HC. Fifteen novel FBN1 mutations causing marfan syndrome detected by heteroduplex analysis of genomic amplicons. *Am J Hum Genet* 1995;57:8–21.
14. Mátyás G, Alonso S, Patrignani A, Marti M, Arnold E, Magyar I, Henggeler C, Carrel T, Steinmann B, Berger W. Large genomic fibrillin-1 (FBN1) gene deletions provide evidence for true haploinsufficiency in Marfan syndrome. *Hum Genet* 2007;122:23–32.
15. Rommel K, Karck M, Haverich A, von Kodolitsch Y, Rybczynski M, Müller G, Singh KK, Schmidtke J, Arslan-Kirchner M. Identification of 29 novel and nine recurrent fibrillin-1 (FBN1) mutations and genotype-phenotype correlations in 76 patients with Marfan syndrome. *Hum Mutat* 2005;26:529–539.
16. Liu WO, Oefner PJ, Qian C, Odom RS, Francke U. Denaturing HPLC-identified novel FBN1 mutations, polymorphisms, and sequence variants in Marfan syndrome and related connective tissue disorders. *Genet Test* 1997;1:237–242.
17. Pepe G, Giusti B, Evangelisti L, Porciani MC, Brunelli T, Giurlani L, Attanasio M, Fattori R, Bagni C, Comeglio P, Abbate R, Gensini GF. Fibrillin-1 (FBN1) gene frameshift mutations in Marfan patients: genotype-phenotype correlation. *Clin Genet* 2001;59:444–450.
18. Loeys B, De Backer J, Van Acker P, Wettinck K, Pals G, Nuytinck L, Coucke P, De Paepe A. Comprehensive molecular screening of the FBN1 gene favors locus homogeneity of classical Marfan syndrome. *Hum Mutat* 2004;24:140–146.
19. Loeys BL, Schwarze U, Holm T, Callewaert BL, Thomas GH, Pannu H, De Backer JF, Oswald GL, Symoens S, Manouvrier S, Roberts AE, Faravelli F, Greco MA, Pyeritz RE, Milewicz DM, Coucke PJ, Cameron DE, Braverman AC, Byers PH, De Paepe AM, Dietz HC. Aneurysm syndromes caused by mutations in the TGFb receptor. *N Engl J Med* 2006;355:788–798.
20. Guo DC, Pannu H, Tran-Fadulu V, Papke CL, Yu RK, Avidan N, Bourgeois S, Estrera AL, Safi HJ, Sparks E, Amor D, Ades L, McConnell V, Willoughby CE, Abuelo D, Willing M, Lewis RA, Kim DH, Scherer S, Tung PP, Ahn C, Buja LM, Raman CS, Shete SS, Milewicz DM. Mutations in smooth muscle alpha-actin (ACTA2) lead to thoracic aortic aneurysms and dissections. *Nat Genet* 2007;39: 1488–1493.
21. Zhu L, Vranckx R, Khau Van Kien P, Lalande A, Boisset N, Mathieu F, Wegman M, Glancy L, Gasc JM, Brunotte F, Bruneval P, Wolf JE, Michel JB, Jeunemaitre X. Mutations in myosin heavy chain 11 cause a syndrome associating thoracic aortic aneurysm/aortic dissection and patent ductus arteriosus. *Nat Genet* 2006;38:343–349.
22. van de Laar IM, Oldenburg RA, Pals G, Roos-Hesselink JW, de Graaf BM, Verhagen JM, Hoedemaekers YM, Willemsen R, Severijnen LA, Venselaar H, Vriend G, Pattynama PM, Collée M, Majoor-Krakauer D, Poldermans D, Frohn-Mulder IM, Micha D, Timmermans J, Hilhorst-Hofstee Y, Bierma-Zeinstra SM, Willems PJ, Kros JM, Oei EH, Oostra BA, Wessels MW, Bertoli-Avella AM. Mutations in SMAD3 cause a syndromic form of aortic aneurysms and dissections with early-onset osteoarthritis. *Nat Genet* 2011;43:121–126.

Expert Opinion

Novel IκB kinase inhibitors for treatment of nuclear factor-κB-related diseases

Jun-ichi Suzuki†, Masahito Ogawa, Susumu Muto, Akiko Itai, Mitsuaki Isobe, Yasunobu Hirata & Ryozo Nagai
†*University of Tokyo, Graduate School of Medicine, Department of Advanced Clinical Science and Therapeutics, Tokyo, Japan*

Introduction: NF-κB is a key regulator of inflammation and immunity in cancer development. The IκB kinase (IKK) is a multisubunit complex containing catalytic subunits termed IKK-α, -β and -γ. It is well known that many pro-inflammatory stimuli require the IKK-β subunit for NF-κB activation.
Areas covered: NF-κB affects the progression of inflammation-related diseases, such as myocardial ischemia, bronchial asthma, arthritis, cancer and other diseases. We review the characteristics and effects of these inhibitors on inflammatory and other diseases.
Expert opinion: Various synthesized IKK inhibitors have been developed and they will be used clinically in the near future.

Keywords: chemical compounds, inflammation, IκB kinase, NF-κB

Expert Opin. Investig. Drugs (2011) 20(3):395-405

1. Introduction

NF-κB is known to be a key factor in the regulation of inflammation [1] and immunity in cancer development [2]. The IκB kinase (IKK) is a multisubunit complex containing catalytic subunits termed IKK-α, -β and -γ [3]. To date, two major NF-κB activation pathways have been elicited based on the ligand interaction with surface receptors. Canonical signaling depends on IKK-γ and -β and induces the transcription of genes that regulate inflammation and cell survival. In contrast, non-canonical NF-κB activation is mostly involved in the regulation of B-cell development [4]. Although both pathways can affect development of inflammation, most of our knowledge relates to the canonical pathway. This pathway is triggered by infections and pro-inflammatory cytokines which activate IKK complex. This complex is composed of two catalytic subunits, IKK-α and -β, and a regulatory subunit, IKK-γ (NF-κB essential modulator; NEMO). The IKK complex phosphorylates NF-κB-bound IκBs, thereby targeting them for proteasomal degradation and liberating NF-κB dimers that are composed of REL-A (known as p65), REL and p50 subunits to enter the nucleus and mediate transcription of target genes. This reaction mostly depends on the catalytic subunit IKK-β, which carries out IκB phosphorylation. The non-canonical pathway involves the upstream kinase NF-κB-inducing kinase leading to the phosphorylation and processing of p100 in response to certain members of the TNF family. The two pathways switch on different gene sets and, therefore, mediate different immune functions. The contribution of the canonical pathway to acute inflammation and cell-survival mechanisms is well accepted, and sustained NF-κB activation in various malignancies has been described. Owing to the variety of target genes of the canonical pathway, which include those encoding mediators of inflammation, cytokines, chemokines, proteases and inhibitors of apoptosis (**Figure 1**), it has been proposed that canonical NF-κB activation might link inflammation to tumor promotion and progression [5].

10.1517/13543784.2011.559162 © 2011 Informa UK, Ltd. ISSN 1354-3784

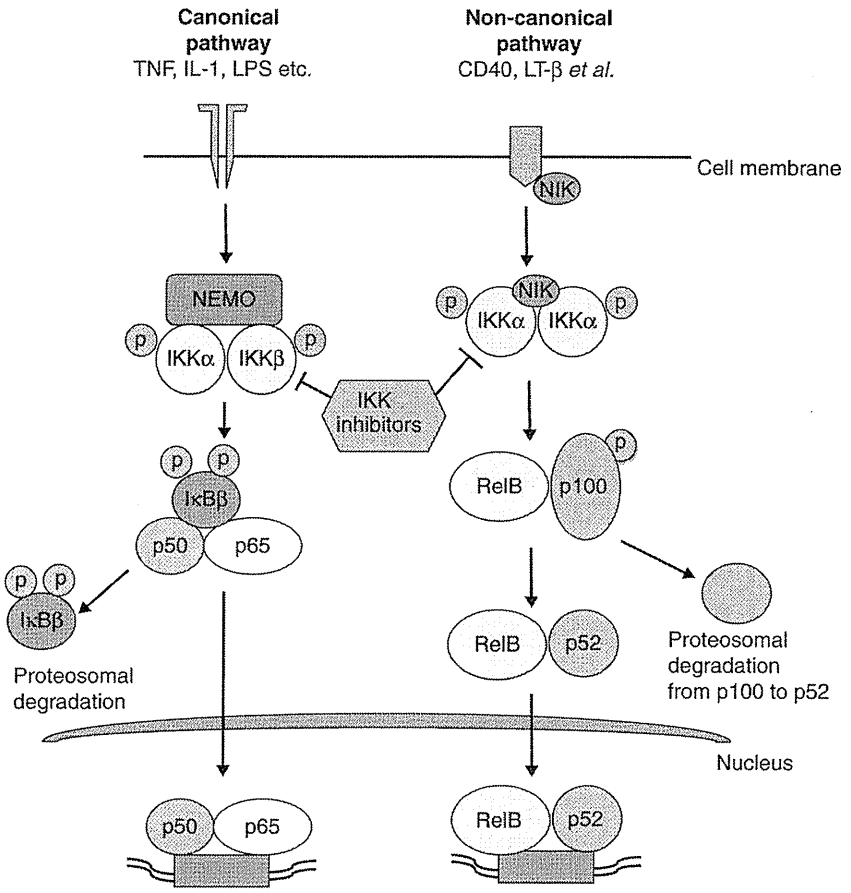

Figure 1. Canonical and non-canonical pathways of NF-κB.

Gene-targeting experiments revealed that many pro-inflammatory stimuli required IKK-β subunit for NF-κB activation [6]. Thus, IKK-deficient mice died in the embryonic or perinatal periods (IKK-$\alpha^{-/-}$, -$\beta^{-/-}$ or -$\gamma^{-/-}$) demonstrating their critical role [7,8]. Dominant-negative IKK-β blocks NF-κB-dependent transcription, while IKK-α plays a role only in response to certain stimuli and in limited cells. Recently, novel synthesized chemical compounds that act as IKK inhibitors have been developed. They are the phosphorylation inhibitors of IκB that act via inhibition of IKK-α and/or -β. To clarify the effects of the inhibitors, we review previous articles on inflammatory diseases.

2. Reagents

IMD-0354 (*N*-(3,5-bis-trifluoromethyl-phenyl)-5-chloro-2-hydroxy-benzamide) [9,10] and IMD-0560 (*N*-(2,5-bis-trifluoromethyl-phenyl)-5-bromo-2-hydroxy-benzamide) [11] were developed as novel IKK inhibitors. They are the phosphorylation inhibitors of IκB that act via inhibition of IKK-β. IMD-0354 (molecular mass, 384.1, **Figure 2A**) was molecular-designed, synthesized and provided by the Institute of Medicinal Molecular Design, Inc. (Tokyo, Japan). The 3D structure of a kinase domain of IKK-β was constructed by homology modeling with protein kinase A as a template. The structure of active IKK-β was estimated by referring to a model of IKK regulation. The molecular structure of IMD-0354 was designed by analyzing a binding mode of aspirin to IKK-β. To investigate the characteristics of IMD-0354, we performed a NF-κB–IKK-β reporter assay with the constitutively active mutant IKK-β. IMD-0354 inhibited the activated expression of NF-κB in a dose-dependent manner in HepG2 cells that were transfected with pFLAG-CMV-IKKh (S177E/S181E) vector. IMD-0354 also decreased the levels of cytosolic phospho-IκBα in TNF-α stimulated cardiomyocytes in a dose-dependent manner. The kinetics of NF-κB translocation was consistent with the degree of phosphorylation of cytosolic IκBα. The translocation was blocked markedly by treatment with IMD-0354. TNF-α-induced production of IL-1α and monocyte chemoattractant protein-1 (MCP-1) from cultured cardiomyocytes were reduced significantly by IMD-0354. Taken together, IMD-0354 inhibits IKK-β, resulting in the blockade of IκBα phosphorylation.

Another IKK inhibitor, IMD-0560 (molecular mass 428.1), was also synthesized and provided by the Institute of Medical

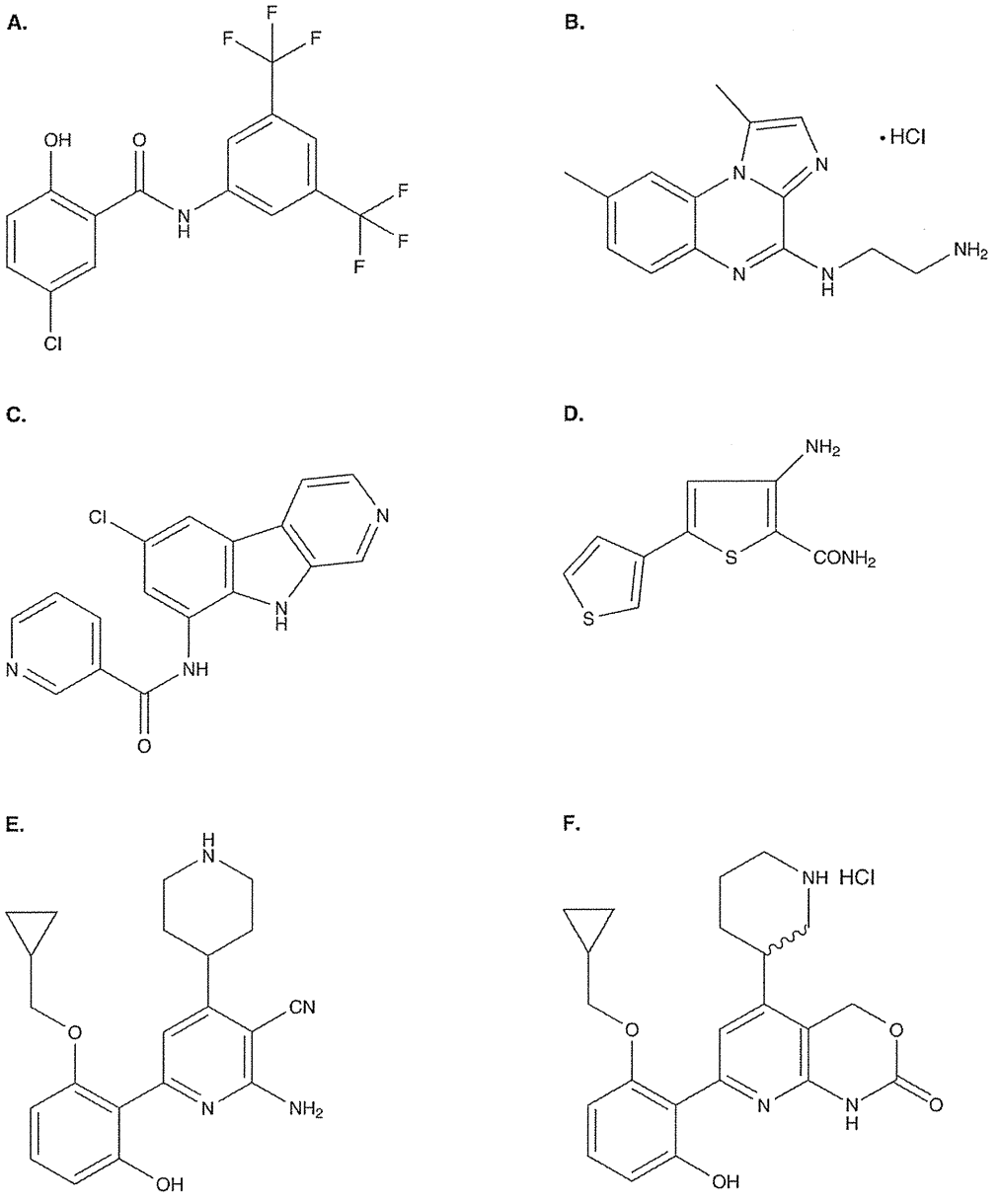

Figure 2. Chemical structures of the chemical compounds A, IMD-0354; B, BMS-345541; C, PS-1145; D, SC-514; E, ACHP and F, Bay 65 - 1942.

Molecular Design using the same methodology of IMD-0354. IMD-0560 inhibited the activated expression of NF-κB in HEK293T cells transfected with the p-FLAG-CMV-IKK-β (S177E/S181E) vector in a dose-dependent manner. Further, pretreatment with IMD-0560 dose-dependently suppressed the DNA binding activity of NF-κB. IMD-0560 also suppressed the nuclear translocation of NF-κB and phosphorylation of IκBα induced by TNF-α in fibroblast-like synoviocytes (FLS). Further, this compound suppressed the production of inflammatory cytokines and chemokines; it also inhibited the proliferation of FLS without showing cellular toxicity [11,12].

BMS-345541, 4(2′-aminoethyl)amino-1,8-dimethylimidazo(1,2-α) quinoxaline, was reported as a highly selective inhibitor of IKK that inhibits NF-κB-dependent transcription of pro-inflammatory cytokines (**Figure 2B**). BMS-345541 was identified as a selective inhibitor of the catalytic subunits of IKK (IKK-β IC_{50} = 0.3 μM, IKK-α IC_{50} = 4 μM). This inhibitor appears to bind to an unidentified allosteric-binding site of the IKK catalytic subunits. The compound failed to inhibit a panel of 15 other kinases and selectively inhibited the stimulated phosphorylation of IκB in cells. It also failed to affect c-Jun and STAT3 phosphorylation, as well as MAPK-2 activation in cells. The compound has good pharmacokinetic

characteristics (oral bioavailability 100%, intravenous half-life 2.2 h), which makes it particularly well suited for use in investigating the utility of IKK inhibitors in disease models [13].

PS-1145, *N*-(6-chloro-9*H*-β-carbolin-8-yl) nicotinamide, was also reported (**Figure 2C**) [14]. The compound PS-1145 was tested for its ability to block the phosphorylation of IκBα in HeLa cells following TNF-α stimulation. Immunoblot analysis showed a dose-dependent inhibition of phosphorylated IκBα. It then evaluated the effects of the compound on NF-κB activation by measuring DNA binding activity after TNF-α treatment in the same HeLa cells. EMSA showed a dose-dependent inhibition of NF-κB activation by the compound. Consistent with the inhibition of NF-κB activation, this compound also blocks the transcription of intracellular adhesion molecule (ICAM)-1 in HUVEC primary cultures [15]. PS-1145 inhibited TNF-α production with an IC_{50} of 4.7 μM/l [16].

SC-514, 5-(thien-3-yl)-3-aminothiophene-2-carboxamide, was identified as another selective IKK inhibitor (**Figure 2D**). This compound does not inhibit other IKK isoforms or other serine–threonine and tyrosine kinases. SC-514 inhibits the native IKK complex or recombinant human IKK-α/-β heterodimer and IKK-β homodimer. IKK-β inhibition by SC-514 is selective, reversible and competitive with ATP. SC-514 has several interesting effects; it does not inhibit the phosphorylation and activation of the IKK complex, and delays but does not completely block IκBα phosphorylation and degradation. Thus, the effect of SC-514 on cytokine gene expression is a combination of inhibiting IκBα phosphorylation/degradation affecting NF-κB nuclear import/export, as well as the phosphorylation and transactivation of p65 [17].

ACHP, 2-amino-6-[2-(cyclopropylmethoxy)-6-hydroxyphenyl] -4-piperidin-4-yl-nicotinonitrile, was developed and evaluated as a potent inhibitor for IKK-α and -β (**Figure 2E**). When massive screening was conducted, ACHP was found to have specific inhibitory action on IKK-α and -β. The IC_{50} values for IKK-α and -β are 8.5 and 250 nmol/l, respectively, measured by *in vitro* kinase assays. ACHP also showed good aqueous solubility and cell permeability, thus, demonstrating high bioavailability in mice and rats [18,19].

Bay 65 – 1942, {7-[2-(cyclopropylmethoxy)-6-hydroxyphenyl]-5-[(3*S*)-3-piperidinyl]-1,4-dihydro-2Hpyrido[2,3-d][1,3]oxazin-2-one hydrochloride}, was composed as an IKK-β inhibitor (**Figure 2F**). Through competitive inhibition of ATP at the IKK-β subunit, Bay 65 – 1942 prevented the phosphorylation of IκBα by the IKK complex [20].

AS602868 is an anilinopyrimidine derivative and ATP competitor, which inhibits IKK-β with an IC_{50} = 62 nmol/l (K_i = 20 nmol/l). The compound showed some inhibitory effect on JNK2. In a series of tests on different cell lines, AS602868 was shown to block phosphorylation of IκB and subsequent NF-κB activation [21].

NEMO binding domain (NBD) peptide was reported as an IKK inhibitor [22]. The specific molecular mechanisms of NEMO–IKK interactions involve a C-terminal hexapeptide core sequence present on both IKK-α and -β. Peptides corresponding to the IKK-β NBD have been found to disrupt the association of recombinant NEMO with recombinant IKK-α or -β *in vitro*. The cell-permeable versions of these peptides blocked NF-κB activation in various cellular and animal models of inflammation [23].

It is well known that some natural products, such as polyphenols, have various effects on IKK inhibition. Pan *et al.* investigated the inhibition of IKK activity in lipopolysaccharide (LPS)-activated murine macrophages by various polyphenols including (-)-epigallocatechin-3-gallate (EGCG) and theaflavin-3,3′-digallate (TF-3). TF-3 inhibited IKK activity in activated macrophages more strongly than the other polyphenols. TF-3 strongly inhibited both IKK-α and -β activity and prevented the degradation of IκBα and IκBβ in activated macrophage cells. The results suggest that the inhibition of IKK activity by TF-3 could occur by a direct effect on IKKs or on upstream events in the signal transduction pathway [24]. Yang *et al.* also revealed that EGCG was a potent IKK inhibitor because EGCG inhibited phosphorylation of IκBα and decreased IKK activity in cytosolic extracts [25].

3. The effects on disease models

3.1 Cardiovascular diseases

Myocardial ischemia reperfusion injury is related closely to inflammatory reactions. Morishita *et al.* revealed that inhibition of NF-κB using decoy oligodeoxynucleotides (ODNs) reduced the extent of myocardial infarction following reperfusion [26]. Thus, we investigated the efficacy of IκB phosphorylation blockade using IMD-0354 in a rat myocardial ischemia/reperfusion injury model [9]. Treatment with IMD-0354 resulted in a significant reduction of the infarction area:area at risk ratio and the preservation of fractional shortening. Histology showed that accumulation of polymorphonuclear neutrophils in the area at risk decreased significantly. *In vitro* study revealed that IMD-0354 inhibited nuclear translocation of NF-κB induced by TNF-α in cultured cardiomyocytes. IMD-0354 caused a significant reduction of chemokine (MCP-1) production in a concentration-dependent manner compared with vehicle-treated cells. Therefore, we concluded that inhibition of nuclear translocation of NF-κB by IMD-0354 could provide an effective approach to attenuate ischemia/reperfusion injury through chemokine suppression. Ventricular remodeling after myocardial infarction is also related to inflammatory reactions. Thus, we studied the effects of IMD-0354 [6] and IMD-0560 [11] in a rat myocardial infarction model. IMD-0354 or IMD-0560 administration reduced plasma brain natriuretic peptide levels after myocardial infarction. Either IMD-0354 or IMD-0560 treatment preserved left ventricular fractional shortening after infarction. Histology

showed that IMD-0354 significantly reduced myocardial macrophage infiltration and fibrosis. Western blot revealed that IMD-0354 suppressed MCP-1 expression in non-infarcted myocardial samples. *In gel* and *in situ* zymography clarified that either IMD-0354 or IMD-0560 treatment significantly suppressed MMP-9 activity in the non-infarcted myocardium. Therefore, we concluded that both IMD-0354 and IMD-0560 significantly affect the prevention of heart failure that is induced by ventricular remodeling after myocardial ischemia via altered MMP activation.

BMS-345541 was tested for its ability to suppress graft rejection in a murine heterotopic cardiac allograft model by Townsend *et al.* The compound did not prolong graft survival when administered at 50 mg/kg as a single agent. However, graft survival was significantly increased when it was administered with a suboptimal dose of cytotoxic T-lymphocyte antigen-4 immunoglobulin or cyclosporine A compared with either agent alone. They concluded that BMS-345541 may serve as a novel adjunctive therapy for the prevention of graft rejection [27].

SC-514 examined the effects using rat aortic smooth muscle cells. SC-514 treated cells significantly reduced iNOS induction, NF-κB DNA binding and IκBα loss. The results suggest that IKK-β plays a predominant, selective role in the regulation of NF-κB-dependent induction of iNOS in smooth muscle cells [28]. SC-514 inhibited all forms of recombinant human IKK-α, including rhIKK-β homodimer, rhIKK-α/-β heterodimer, as well as the constitutively active form of rhIKK-β with comparable IC_{50} values in the 3 – 12 μM range [29].

Moss *et al.* also reported that Bay 65 – 1942 can provide both acute and chronic cardioprotection and offers a clinically accessible target for preventing cardiac injury following ischemia reperfusion [30].

We demonstrated that tea catechins suppressed several cardiovascular diseases. We performed oral administration of catechins into murine and rat models of cardiac transplantation [31], myocarditis [32], myocardial ischemia [33] and atherosclerosis [34] to reveal the effects of catechins on the inflammation-induced ventricular and arterial remodeling. From our results, catechins are potent agents for the treatment and prevention of inflammation-related cardiovascular diseases, as they are critically involved in the suppression of pro-inflammatory signaling pathways.

3.2 Lung injury

NF-κB plays a key role in the progression of lung injury. Matsuda *et al.* revealed that NF-κB decoy ODNs prevented acute lung injury in mice [35]. Thus, we examined the effects of IMD-0354 to attenuate bleomycin-induced pulmonary fibrosis in mice [36]. IMD-0354 reduced the collagen content and fibrotic scores in the mice that received bleomycin. The bronchoalveolar lavage demonstrated that the proportions of neutrophils and lymphocytes decreased in mice treated with IMD-0354. The results suggested that IMD-0354 might be useful to ameliorate inflammation in the lungs induced by chemical injury.

BMS-345541 is also known to affect acute lung injury. Everhart *et al.* administered BMS-345541 to determine whether intervention in the NF-κB pathway could prevent progression of lung injury in the LPS pump model. They revealed that treatment with BMS-345541 reduced lung NF-κB activation, concentration of pro-inflammatory cytokines and chemokines in lung lavage, neutrophil influx and lung edema. Therefore, they concluded that sustained NF-κB activation correlates with severity of lung injury and that BMS-345541 is beneficial to suppress lung inflammation [37]. PS-1145 also tested the effects using human ASM cells and pulmonary epithelial cells *in vitro*. As observed in human ASM cells, PS-1145 reduced expression of several adhesion molecules, cytokines and chemokines [38]. Similarly, PS-1145 reduced NF-κB-dependent transcription induced by IL-1β and TNF-α in primary pulmonary epithelial cells [39]. Chapoval *et al.* revealed the *in vivo* effects of PS-1145 using IL-13 transgenic mice. While IL-13 induced tissue inflammation, fibrosis and alveolar remodeling, PS-1145 inhibited lung inflammatory and structural cell apoptosis with suppression of caspase activation [40].

3.3 Arthritis

Rheumatoid arthritis (RA) is affected by NF-κB activation. Tomita *et al.* showed that NF-κB decoy ODN suppressed the severity of collagen-induced arthritis in rats [41]. Thus, we evaluated the effect of IMD-0560 on collagen type II-induced arthritis in mice [12]. In this investigation, IMD-0560 suppressed the nuclear translocation of NF-κB and phosphorylation of IκB induced by TNF-α. In addition, this compound suppressed the production of inflammatory cytokines, including IL-6 and -8. IMD-0560 was effective against collagen-induced arthritis in mice via suppression of pro-inflammatory cytokines. Thus, we concluded that IMD-0560 could be a new therapeutic agent for RA.

BMS-345541 intensively evaluated the effects on RA. McIntyre *et al.* revealed that BMS-345541 is efficacious against collagen-induced arthritis in mice. BMS-345541 reduced the incidence of disease, inhibiting clinical signs of disease. Histological evaluation of the joints showed that BMS-345541 blocked inflammation and joint destruction. Transcription levels of IL-1 in the joints were also inhibited in the mice that received BMS-345541 [42]. Pattoli *et al.* also examined whether BMS-345541 directly inhibits cytokine-induced metalloproteinase expression and cartilage degradation. BMS-345541 inhibited IL-1-dependent expression of MMP-1, -3 and -13 in chondrosarcoma cells. Thus, BMS-345541 blocks collagen degradation through suppression of metalloproteinase expression [43].

Jimi *et al.* also revealed that the NBD peptide inhibited RANKL-stimulated NF-κB activation and osteoclastogenesis both *in vitro* and *in vivo*. This peptide significantly reduced the severity of collagen-induced arthritis in mice by reducing